

Renormalization group evolution of neutrino masses and mixing in seesaw models: A review

Shamayita Ray*

*Institute for High Energy Phenomenology,
Newman Laboratory of Elementary Particle Physics,
Cornell University, Ithaca, NY 14853, USA*

May 13, 2010

Abstract

We consider different extensions of the standard model which can give rise to the small active neutrino masses through seesaw mechanisms, and their mixing. These tiny neutrino masses are generated at some high energy scale by the heavy seesaw fields which then get sequentially decoupled to give an effective dimension-5 operator. The renormalization group evolution of the masses and the mixing parameters of the three active neutrinos in the high energy as well as the low energy effective theory is reviewed in this article.

*Electronic address: sr643@cornell.edu

Alternative electronic address: shamayitar@theory.tifr.res.in

Contents

1	Introduction	3
1.1	Neutrino oscillations: The current status	3
1.2	Absolute masses of the active neutrinos	5
1.3	RG evolution of neutrino parameters	7
2	Generation of light neutrino masses	7
2.1	Low energy effective theory of neutrino masses	7
2.2	High energy theories: Seesaw mechanisms	8
2.2.1	Type-I seesaw	9
2.2.2	Type-II seesaw	12
2.2.3	Type-III seesaw	14
2.2.4	Inverse seesaw	17
3	RG evolution of neutrino masses and mixing in effective theories	18
3.1	Evolution equations for neutrino parameters from matrix equations	20
3.1.1	RG evolution of the mixing angles and phases	21
3.1.2	RG evolution of the light neutrino masses	22
3.1.3	A subtlety at $\theta_{13} = 0$	25
4	RG evolution of neutrino masses and mixing in high energy seesaw models	27
4.1	Sequential decoupling of heavy fields	29
4.2	RG evolution of neutrino mixing parameters	35
4.2.1	Evolution of mixing angles	35
4.2.2	Evolution of $J_{\text{CP}}, J'_{\text{CP}}$	39
4.2.3	Evolution of Majorana phases	40
4.2.4	Evolution of light neutrino masses	41
4.2.5	Contribution from U_e	42
5	Conclusions	45
	Appendix: Diagonalization of neutrino mass matrix	46
	Bibliography	47

1 Introduction

1.1 Neutrino oscillations: The current status

The field of neutrino physics has made immense progress in the last decade, which was initiated when the Super-Kamiokande (SK) experiment in Japan [1] reported the evidence for oscillations in the atmospheric neutrinos. Now there is compelling evidence that solar, atmospheric, accelerator and reactor neutrinos oscillate, which implies that the neutrinos are massive and the leptons mix among themselves.

The atmospheric neutrinos are produced in the Earth's atmosphere by cosmic rays. The flux of cosmic rays that lead to neutrinos with energies above a few GeV is isotropic. Hence one expects the downward and the upward-going fluxes of multi-GeV neutrinos of a given flavor to be equal. The underground SK detector found that for multi-GeV atmospheric muon neutrinos the zenith-angle dependence deviates from this expectation and the deviation can be explained when one invokes $\nu_\mu \rightarrow \nu_\tau$ oscillations. The oscillations of muon neutrinos into other flavors have also been confirmed by the energy spectrum obtained from the controlled source experiments K2K [2] and MINOS [3]. The allowed region for the oscillation parameters, Δm_{atm}^2 and $\sin^2 2\theta_{\text{atm}}$, is shown in Fig 1(a).

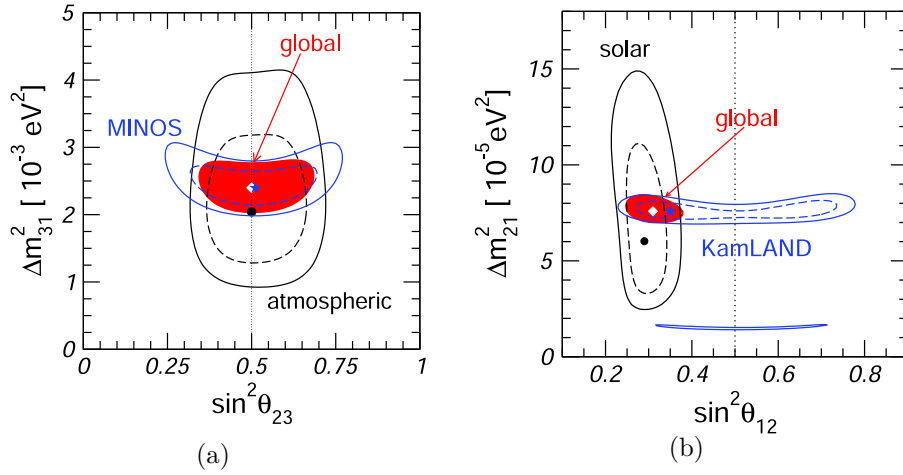


Figure 1: (a) The region of the atmospheric oscillation parameters Δm_{atm}^2 and $\sin^2 2\theta_{\text{atm}}$ obtained from the SK, K2K and MINOS experiments [4]; (b) The allowed region in the neutrino oscillation parameter space from solar neutrino data and KamLAND experiment [4].

As can be seen from the figure, the MINOS data is capable of measuring Δm_{atm}^2 with high precision, while SK put stronger bound on $\sin^2 2\theta_{\text{atm}}$. The results from the short-baseline (SBL) experiments (like CDHS [6], NOMAD [7] etc.) show that the $\nu_\mu \rightarrow \nu_e$ oscillations can be present only as small sub-dominant effects and also put strong bounds on the active-sterile mixing angles in $\nu_\mu \rightarrow \nu_s$ oscillations, an oscillation channel whose sub-dominant effect is not yet ruled out completely.

The pioneering solar neutrino experiment by Davis and collaborators using ^{37}Cl reported a solar electron neutrino flux significantly smaller than that predicted by the standard solar model, and this deficit in the number of electron neutrinos is known as the “solar neutrino problem”. The puzzle persisted in the literature for about 30 years, and then the charged current (CC) and the neutral current (NC) data from the SNO experiment [8], combined with the SK solar neutrino data [9], provided direct evidence for neutrino oscillations in solar neutrinos. However, four different solutions were there to explain the solar neutrino oscillations [10]: (i) the LMA or large mixing angle solution ($\Delta m_\odot^2 = 5.0 \times 10^{-5} \text{ eV}^2$, $\tan^2 \theta_\odot = 0.42$), (ii) the low mass solution ($\Delta m_\odot^2 = 7.9 \times 10^{-8} \text{ eV}^2$, $\tan^2 \theta_\odot = 0.61$), (iii) the vacuum solution ($\Delta m_\odot^2 = 4.6 \times 10^{-10} \text{ eV}^2$, $\tan^2 \theta_\odot = 1.8$) and (iv) the SMA or small mixing angle solution ($\Delta m_\odot^2 = 5.0 \times 10^{-6} \text{ eV}^2$, $\tan^2 \theta_\odot = 1.5 \cdot 10^{-3}$). The results from the controlled source experiment KamLAND [11] confirmed the LMA solution and ruled out the other three possibilities. Fig 1(b) shows the allowed region of the solar neutrino oscillation parameters Δm_\odot^2 and $\tan^2 \theta_\odot$.

Combining the results obtained from the solar, atmospheric and the reactor neutrino oscillation experiments described above, the current knowledge about the neutrinos is that there are three neutrino flavors ($\nu_\alpha, \alpha \in \{e, \mu, \tau\}$) which mix to form three neutrino mass eigenstates ($\nu_i, i \in \{1, 2, 3\}$). These mass eigenstates are separated by $\Delta m_{ij}^2 \equiv m_i^2 - m_j^2$ where, $m_{i,j}$ denote mass eigenvalues with $i, j \in \{1, 2, 3\}$. The two sets of eigenstates are connected through $\nu_\alpha = (U_{\text{PMNS}})_{\alpha i} \nu_i$, where U_{PMNS} is the Pontecorvo-Maki-Nakagawa-Sakata neutrino mixing matrix [12, 13, 14, 15] in the basis where the charged lepton mass matrix is diagonal. This mixing matrix is parametrized as

$$U_{\text{PMNS}} = P \cdot \mathcal{U} \cdot Q, \quad (1)$$

where

$$\mathcal{U} = U_{23}(\theta_{23}, 0) U_{13}(\theta_{13}, \delta) U_{12}(\theta_{12}, 0), \quad Q = \text{Diag}\{e^{-i\phi_1}, e^{-i\phi_2}, 1\}. \quad (2)$$

Here $U_{ij}(\theta, \delta)$ is the complex rotation matrix in the i - j plane, δ is the Dirac CP violating phase, ϕ_i are the Majorana phases, and P is the flavor phase matrix (Sometimes the flavor phases are called as the unphysical phases since

	Best fit	3σ range
Δm_{21}^2 [10^{-5}eV^2]	7.65	7.05 - 8.34
$ \Delta m_{31}^2 $ [10^{-3}eV^2]	2.40	2.07 - 2.75
$\sin^2 \theta_{12}$	0.304	0.25 - 0.37
$\sin^2 \theta_{23}$	0.50	0.36 - 0.67
$\sin^2 \theta_{13}$	0.01	≤ 0.056

Table 1: The present best-fit values and 3σ ranges of oscillation parameters [4, 16, 17].

they do not play any role in the phenomenology of neutrino mixing or beta-decay.) Finally, with all the above definitions, \mathcal{U} takes the form

$$\mathcal{U} = \begin{pmatrix} c_{12}c_{13} & s_{12}c_{13} & s_{13}e^{-i\delta} \\ -c_{23}s_{12} - s_{23}s_{13}c_{12}e^{i\delta} & c_{23}c_{12} - s_{23}s_{13}s_{12}e^{i\delta} & s_{23}c_{13} \\ s_{23}s_{12} - c_{23}s_{13}c_{12}e^{i\delta} & -s_{23}c_{12} - c_{23}s_{13}s_{12}e^{i\delta} & c_{23}c_{13} \end{pmatrix}, \quad (3)$$

where c_{ij} and s_{ij} are the cosines and sines respectively of the mixing angle θ_{ij} . The current best-fit values and 3σ ranges of these parameters are summarized in Table 1. It is still not known whether the neutrino mass ordering is normal ($m_1 < m_2 < m_3$) or inverted ($m_3 < m_1 < m_2$). Many other high precision oscillation experiments are going on and also being planned in order to measure the neutrino oscillation parameters with higher accuracy and to determine the neutrino mass ordering.

As can be seen from the PMNS parametrization of the neutrino mixing matrix in Eq. (3), the angle θ_{13} plays a crucial role in the determination of the Dirac CP phase δ . As shown in the Table 1, θ_{13} can also be consistent with zero at 3σ . However, this data also implies that assuming the error to scale linearly upto 3σ within the physical range of $\sin^2 \theta_{13}$, there is a hint of $\theta_{13} > 0$ at $\sim 0.9\sigma$. It has been shown that the solar and KamLAND data implies a non-zero θ_{13} at $\sim 1.5\sigma$ [18, 19]. But when combined with atmospheric, long-baseline reactor and CHOOZ data, the significance is lowered since the hint for a non-zero θ_{13} from the atmospheric data is not so robust and depends on the details of event rate calculations and the treatment of theoretical uncertainties [18].

1.2 Absolute masses of the active neutrinos

While the neutrino oscillation experiments are not sensitive to the absolute neutrino masses, the beta decay and the neutrinoless double beta decay ($0\nu\beta\beta$) processes are. At the same time, it is possible to estimate $\sum_i m_i$

from cosmology also. In case of beta decay, the non-zero neutrino mass would modify the Kurie plot, regardless of whether the neutrinos are Dirac or Majorana particles. The effect will depend on $m_\beta = (\sum_i |U_{ei}|^2 m_i^2)^{1/2}$, and if the neutrino masses are small, it will be visible only near the end point of the Kurie plot. The Mainz [20] experiment has placed the upper limit of $m_\beta \leq 2.3$ eV. The upcoming beta-decay experiments like KATRIN [21] will be sensitive to $m_\beta > 0.2$ eV and will thus improve the bound by an order of magnitude. The $0\nu\beta\beta$ decay, on the other hand, is sensitive to the effective Majorana mass of the electron neutrinos, defined as $m_{ee} \equiv |\sum_i U_{ei}^2 m_i|$, and will be observed only if the neutrinos are Majorana particles. A non-zero signal for the $0\nu\beta\beta$ decay will put bound on the specific combination of the neutrino masses and the Majorana phases given by m_{ee} . The current limit put by the Heidelberg-Moscow experiment [22] is $m_{ee} \lesssim 0.9$ eV. The cosmic microwave background radiation (CMBR) carries the imprint of the neutrino masses since in the standard Big Bang model, for the standard model (SM) interactions of the neutrinos, the neutrinos are abundant like the photons till the epoch of nucleosynthesis when they decouple from the thermal bath of the photons. It is also possible to get information about the neutrino masses from the study of the large scale structure as an active neutrino species of mass m_ν will tend to wash out all structures upto a scale $\sim 1/m_\nu$ by free-streaming. Recent results from the Wilkinson Microwave Anisotropy Probe (WMAP) and the surveys on the large scale structure put the limit $\sum_i m_i \leq 0.67 - 2.0$ eV [23, 24].

The very fact that the active neutrinos are massive demands an extension of the SM. In the framework of the SM, since there is no right-handed neutrino, the neutrinos are massless at the tree-level, and they cannot have a Dirac mass even at loop level. So the only other possibility is the lepton number violating Majorana mass term. But lepton number is a symmetry of the SM, though accidental, and if that symmetry is to be obeyed, Majorana masses also cannot be generated at loop level. It can also be seen that the Planck scale (M_{Pl}) effect cannot introduce the required neutrino mass in the SM as it can only generate a neutrino mass $\sim \mathcal{O}(v_{EW}^2/M_{\text{Pl}}) \approx \mathcal{O}(10^{-5}\text{eV})$, and hence cannot explain the atmospheric mass squared difference. Hence generally the neutrino masses are incorporated at the tree-level by adding new fields to the SM at high energy scales. The most favored mechanisms to generate such small neutrino masses are the so called seesaw mechanisms which need the introduction of one or more heavy fields, while maintains the $\text{SU}(3)_C \times \text{SU}(2)_L \times \text{U}(1)_Y$ gauge group structure of the SM. There are also other models like Inverse seesaw [25], the model with a singly charged singlet proposed originally by Zee [26, 27], the model with a doubly charged singlet

[27, 28], etc. Recently another new model has been proposed in [29], where a pair of vector like leptons and also a Higgs quadruplet are added to the SM to generate neutrino mass. However, some models, like the Zee's model, cannot predict neutrino mixing parameters consistent with the current data. We will discuss some of these models of neutrino masses in detail in Section 2.

1.3 RG evolution of neutrino parameters

Since the neutrino mass is generated at the high scale while the neutrino masses and mixing parameters are measured experimentally at a low scale, the renormalization group (RG) evolution effects need to be included. The current experimental data in Table 1 shows that in the neutrino sector two of the three mixing angles are large, while the third one is small, which is rather different from the quark sector where all three mixing angles are small. Because of the large values of the two mixing angles, RG evolution of the neutrino masses and the mixing parameters plays an important role in the neutrino sector, which is not the case with the quark sector. RG evolution will be even larger if the neutrinos happen to be quasi-degenerate.

The radiative corrections in different theories of neutrino masses are expected to be different since the heavy particles couple differently to the SM fields present. However below the mass scale of the lightest of the heavy particles the effect of all heavy degrees of freedom are integrated out to get an effective theory of neutrino masses. The RG evolution of neutrino masses and mixing parameters in the low energy effective theory as well as in different high energy theories will be discussed in Section 3 and Section 4 respectively.

2 Generation of light neutrino masses

2.1 Low energy effective theory of neutrino masses

The low energy effective Lagrangian needed to explain the non-zero active neutrino masses can in general be expressed as a series of non-renormalizable operators, the dominant one being the dimension-5 operator given as [30]

$$\mathcal{L}_\kappa \sim \kappa_5 l_L l_L \phi \phi . \quad (4)$$

where l_L and ϕ are respectively the lepton and Higgs doublets belonging to the SM. Here κ_5 is the effective coupling which can be expressed in terms of a dimensionless coupling a_5 as $\kappa_5 = a_5/\Lambda$ with Λ some high energy scale. In this picture the SM serves as an effective theory valid upto the mass scale Λ , which can be taken to be the mass of the lightest of the heavy fields.

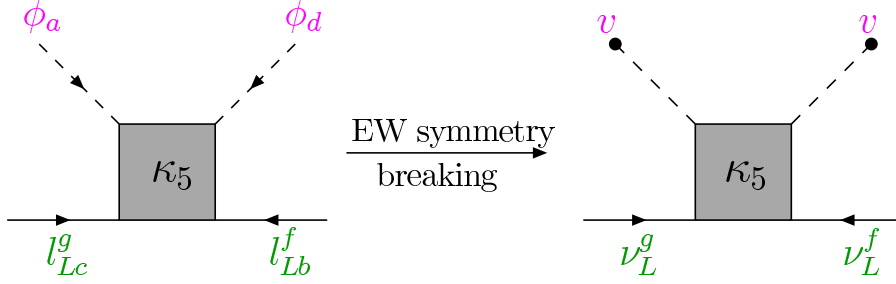


Figure 2: Generation of the Majorana neutrino mass from the low energy effective Lagrangian given in Eq. (4) after spontaneous symmetry breaking.

However, the specific form of κ_5 will depend on the high energy field content and the interactions present at the high scale. The operator shown in Eq. (4) violates lepton number by two units and gives rise to Majorana masses for neutrinos after spontaneous symmetry breaking, $m_\nu \sim \frac{1}{2}\kappa_5 v^2$, as shown in the Fig. 2. Here v is the vacuum expectation value (vev) of the Higgs field ϕ such that

$$\phi = \begin{pmatrix} \phi^+ \\ \phi^0 \end{pmatrix} \xrightarrow[\text{symmetry breaking}]{\text{Spontaneous}} \begin{pmatrix} 0 \\ \frac{v}{\sqrt{2}} \end{pmatrix}. \quad (5)$$

Taking $v \sim 246$ GeV, a neutrino mass of ~ 0.05 eV implies $\Lambda \sim 10^{15}$ GeV if $a_5 \sim 1$.

2.2 High energy theories: Seesaw mechanisms

There are four possible ways to form a dimension-5 gauge singlet term as given in Eq. (4) at low energy through the tree-level exchange of a heavy particle at the high energy: (i) each l_L - ϕ pair forms a fermion singlet, (ii) each of the l_L - l_L and ϕ - ϕ pair forms a scalar triplet, (iii) each l_L - ϕ pair forms a fermion triplet, and (iv) each of the l_L - l_L and ϕ - ϕ pair forms a scalar singlet. Case (i) can arise from the tree-level exchange of a right handed fermion singlet and this corresponds to the Type-I seesaw mechanism [31, 32, 33, 34, 35]. Case (ii) arises when the heavy particle is a Higgs triplet giving rise to the Type-II seesaw mechanism [37, 38]. For case (iii) the exchanged particle should be a right-handed fermion triplet, which corresponds to the Type-III seesaw mechanism [39, 40]. The last scenario gives terms only of the form $\overline{\nu}_L^C e_L$, which cannot generate a neutrino mass. We describe the three different seesaw mechanisms in Section 2.2.1–2.2.3 in detail. A summary of the form of κ and hence the effective light neutrino mass at the low scale in different types of seesaw is given at the end of this section in Table 2. There

is another model, similar to the seesaw models, that can predict the light active neutrino masses and known as the inverse seesaw model. This model will be discussed in Sec 2.2.4, for the sake of completeness.

2.2.1 Type-I seesaw

The simplest extension of the SM to incorporate small active neutrino mass is to introduce right-handed singlet fermions N_R in the theory, which are singlets under the SM gauge group. Hence these N_R fields are essentially right-handed neutrinos. Presence of these new fields allows new terms in the Lagrangian

$$\mathcal{L}_N = \frac{1}{2}\overline{N}(i\partial\!\!\!/)N - \frac{1}{2}\overline{N}\mathbb{M}_N N - \left(\overline{N}Y_N\tilde{\phi}^\dagger l_L + \text{h.c.}\right), \quad (6)$$

where l_L and $\tilde{\phi}$ are respectively the lepton and Higgs doublets belonging to the SM and $\tilde{\phi} \equiv i\sigma^2\phi^*$, σ^2 being the second Pauli matrix. Here we do not write the generation or the $SU(2)_L$ indices explicitly. The field N is defined as $N \equiv N_R + N_R^C$, where N_R^C is the CP conjugate of the right-handed field N_R . Y_N is the Yukawa coupling for the singlet fermion and \mathbb{M}_N is the mass matrix. Thus the complete Lagrangian of the theory becomes

$$\mathcal{L} = \mathcal{L}_{\text{SM}} + \mathcal{L}_N, \quad (7)$$

and after spontaneous symmetry breaking it is possible to write the neutrino mass terms as

$$-\mathcal{L}_{\nu_{\text{mass}}} = \frac{1}{2} \begin{pmatrix} \overline{\nu}_L & \overline{N_R^C} \end{pmatrix} \begin{pmatrix} 0 & \mathbb{m}_D \\ \mathbb{m}_D^T & \mathbb{M}_N \end{pmatrix} \begin{pmatrix} \nu_L^C \\ N_R \end{pmatrix} + \text{h.c.}, \quad (8)$$

where

$$\mathbb{m}_D = (v/\sqrt{2})Y_N^T \quad (9)$$

is the Dirac mass matrix for the neutrinos generated after the electroweak symmetry breaking when the Higgs gets the vev v , as given in Eq. (5). Thus the complete mass matrix for the neutrinos becomes

$$\mathcal{M}_\nu = \begin{pmatrix} 0 & \mathbb{m}_D \\ \mathbb{m}_D^T & \mathbb{M}_N \end{pmatrix}, \quad (10)$$

which when block-diagonalized gives the eigenvalues (see Appendix for derivation)

$$\mathbb{m}_1 \approx -\mathbb{m}_D \mathbb{M}_N^{-1} \mathbb{m}_D^T, \quad (11)$$

$$\mathbb{m}_2 \approx \mathbb{M}_N, \quad (12)$$

	The effective vertex	κ
Type-I		$\kappa = 2Y_N^T M_N^{-1} Y_N$
Type-II		$\kappa = -2 \frac{Y_\Delta \Lambda_6}{M_\Delta^2}$
Type-III		$\kappa = 2Y_\Sigma^T M_\Sigma^{-1} Y_\Sigma$

Table 2: Summary of the low energy effective couplings and the effective neutrino mass $m_\nu \equiv -\frac{v^2}{4}\kappa$ in the three seesaw scenarios. Here, $Y_N(Y_\Sigma)$ are the Yukawa couplings for the heavy singlet(triplet) fermion present in Type-I(Type-III) seesaw and $M_N(M_\Sigma)$ is the mass matrix ($N \equiv N_R + N_R^C$; $\Sigma \equiv \Sigma_R + \Sigma_R^C$). In Type-II seesaw, M_Δ is the mass of the heavy triplet Higgs, Y_Δ is its Yukawa coupling with the SM lepton doublet l_L , and Λ_6 is its coupling with the SM Higgs ϕ .

where we have assumed that $M_N \gg m_D$, *i.e.* the eigenvalues of M_N are much larger than the eigenvalues of m_D and kept terms upto $\mathcal{O}(m_D/M_N)$. Thus Eqs. (12) and (11) show respectively that eigenvalues of the matrix m_2 are large, while those of m_1 are small and hence the eigenstates corresponding to these small eigenvalues should serve the purpose of the mass eigenstates of the light active neutrinos. Thus the presence of the heavy right-handed neutrinos will produce the light active neutrino masses and this mechanism of making one particle light at the expense of making another one heavy is called the seesaw mechanism. The seesaw obtained by adding these heavy right-handed singlet fermions to the SM is called the Type-I seesaw.

In the low energy limit we have an effective theory described by [30]

$$\mathcal{L}_\kappa = \kappa_{fg} \left(\overline{l}_L^C \sigma^i \varepsilon \phi \right) \left(\phi^T \sigma^i \varepsilon l_L^g \right) + \text{h.c.}, \quad (13)$$

$$= -\kappa_{fg} \left(\overline{l}_{Lc}^C \phi_a l_{Lb}^g \phi_d \right) \frac{1}{2} (\varepsilon_{ac} \varepsilon_{bd} + \varepsilon_{ab} \varepsilon_{cd}) + \text{h.c.} , \quad (14)$$

where κ is a symmetric complex matrix with mass dimension (-1) and $\varepsilon \equiv i\sigma^2$ is the completely anti-symmetric tensor in the $\text{SU}(2)_L$ space. Generation indices $f, g \in \{1, 2, 3\}$ are shown explicitly and $a, b, c, d \in \{1, 2\}$ are the $\text{SU}(2)_L$ indices. In writing Eq. (14) we have used

$$\begin{aligned} (\sigma^i)_{ab} (\sigma^i)_{cd} &= 2\delta_{ad} \delta_{bc} - \delta_{ab} \delta_{cd} \\ \Rightarrow (\sigma^i \varepsilon)_{ba} (\sigma^i \varepsilon)_{dc} &= 2\varepsilon_{da} \varepsilon_{bc} - \varepsilon_{ba} \varepsilon_{dc} \end{aligned} \quad (15)$$

and utilizing the $\phi_d \leftrightarrow \phi_a$ symmetry, we can write

$$2\varepsilon_{da} \varepsilon_{bc} - \varepsilon_{ba} \varepsilon_{dc} = \frac{1}{2} (\varepsilon_{ab} \varepsilon_{dc} + \varepsilon_{db} \varepsilon_{ac}) . \quad (16)$$

The relevant diagrams in the complete theory giving rise to the effective operators in the low energy limit are shown in the topmost row in the Table 2. The “shaded box” on the left hand side of the equivalence in the middle column represents the effective low energy vertex κ , while $\mathcal{A}_{(a)}$ and $\mathcal{A}_{(b)}$ are the amplitudes of the diagrams labeled as (a) and (b) on the right hand side. The amplitudes are given by

$$\mathcal{A}_{(a)} = i\mu^\epsilon (Y_N^T \mathbb{M}_N^{-1} Y_N)_{fg} \varepsilon_{ca} \varepsilon_{bd} P_L , \quad (17)$$

$$\mathcal{A}_{(b)} = i\mu^\epsilon (Y_N^T \mathbb{M}_N^{-1} Y_N)_{fg} \varepsilon_{cd} \varepsilon_{ba} P_L , \quad (18)$$

with $\epsilon = 4 - D$ where D is the dimensionality that we introduce in order to use dimensional regularization. Note that $\mathcal{A}_{(b)}$ is obtained from $\mathcal{A}_{(a)}$ just by $d \leftrightarrow a$ interchange. Using Eq. (15) one finally gets

$$\mathcal{A}_{(a)} + \mathcal{A}_{(b)} = -i\mu^\epsilon (Y_N^T \mathbb{M}_N^{-1} Y_N)_{fg} (\varepsilon_{ab} \varepsilon_{cd} + \varepsilon_{ac} \varepsilon_{bd}) P_L . \quad (19)$$

This is equal to the left hand side of the figure mentioned with the identification

$$\kappa = 2Y_N^T \mathbb{M}_N^{-1} Y_N , \quad (20)$$

as shown in the Table 2. From Eqs. (14) and (20), one gets the neutrino mass after spontaneous symmetry breaking to be

$$\mathbb{m}_\nu = -\frac{v^2}{2} Y_N^T \mathbb{M}_N^{-1} Y_N \quad (21)$$

which is the Type-I seesaw relation. As the energy changes, the heavy singlets get decoupled one by one at their respective mass scales and start contributing to the light neutrino mass through the effective operator.

2.2.2 Type-II seesaw

In the Type-II seesaw, we consider the SM extended by a charged Higgs triplet transforming in the adjoint representation of $SU(2)_L$

$$\Delta = \frac{\sigma^i \Delta^i}{\sqrt{2}} = \begin{pmatrix} \Delta^+/\sqrt{2} & \Delta^{++} \\ \Delta^0 & -\Delta^+/\sqrt{2} \end{pmatrix}, \quad (22)$$

where $\Delta^{++} \equiv (\Delta^1 - i\Delta^2)/\sqrt{2}$, $\Delta^0 \equiv (\Delta^1 + i\Delta^2)/\sqrt{2}$ and $\sigma^i \equiv \{\sigma^1, \sigma^2, \sigma^3\}$ are the Pauli matrices. Following the notation of [41, 42], the Lagrangian is given by

$$\mathcal{L} = \mathcal{L}_{\text{SM}} + \mathcal{L}_{\Delta}, \quad (23)$$

where

$$\mathcal{L}_{\Delta} = \mathcal{L}_{\Delta, \text{kin}} + \mathcal{L}_{\Delta, \phi} + \mathcal{L}_{\Delta, \text{Yukawa}}. \quad (24)$$

Here

$$\mathcal{L}_{\Delta, \text{kin}} = \text{Tr} \left[(D_{\mu} \Delta)^{\dagger} D^{\mu} \Delta \right], \quad (25)$$

$$\begin{aligned} \mathcal{L}_{\Delta, \phi} = & -M_{\Delta}^2 \text{Tr} (\Delta^{\dagger} \Delta) - \frac{\Lambda_1}{2} [\text{Tr} (\Delta^{\dagger} \Delta)]^2 \\ & - \frac{\Lambda_2}{2} \left[[\text{Tr} (\Delta^{\dagger} \Delta)]^2 - \text{Tr} (\Delta^{\dagger} \Delta \Delta^{\dagger} \Delta) \right] - \Lambda_4 \phi^{\dagger} \phi \text{Tr} (\Delta^{\dagger} \Delta) \\ & - \Lambda_5 \phi^{\dagger} [\Delta^{\dagger}, \Delta] \phi - \left[\frac{\Lambda_6}{\sqrt{2}} \phi^T i \sigma_2 \Delta^{\dagger} \phi + \text{h.c.} \right], \end{aligned} \quad (26)$$

$$\mathcal{L}_{\Delta, \text{Yukawa}} = -\frac{1}{\sqrt{2}} (Y_{\Delta})_{fg} \ell_L^{Tf} C(i\sigma_2) \Delta \ell_L^g + \text{h.c.}, \quad (27)$$

where C is the charge conjugation matrix with respect to the Lorentz group. The covariant derivative of the Higgs triplet is given by ¹

$$D_{\mu} \Delta = \partial_{\mu} \Delta + i\sqrt{\frac{3}{5}} g_1 B_{\mu} \Delta + ig_2 [W_{\mu}, \Delta], \quad (28)$$

where g_1 and g_2 are the $U(1)_Y$ and $SU(2)_L$ gauge couplings respectively. With the interactions shown in Eqs. (24)–(27), after electroweak symmetry breaking the triplet Higgs Δ will get a vev given by $\langle \Delta_0 \rangle \sim \Lambda_6 v^2 / 2\sqrt{2} M_{\Delta}^2$. This triplet Higgs vev will also contribute to the gauge boson masses and

¹ We use GUT charge normalization: $\frac{3}{5} (g_1^{\text{GUT}})^2 = (g_1^{\text{SM}})^2$.

will alter the ρ -parameters from the SM prediction $\rho \approx 1$, at tree level and hence will get a strong constraint from the current precision data [44].

Once the triplet Higgs Δ gets its vev after spontaneous symmetry breaking, the Lagrangian in Eq. (27) produces the neutrino mass term as

$$\mathcal{L}_{\Delta, Yukawa} = \frac{1}{\sqrt{2}} Y_{\Delta} \nu_L^C \langle \Delta_0 \rangle \nu_L + \text{h.c.} , \quad (29)$$

and thus using the expression for $\langle \Delta_0 \rangle$, the neutrino mass is given as

$$\mathfrak{m}_{\nu} = \frac{v^2}{2} \frac{\Lambda_6 Y_{\Delta}}{\mathbb{M}_{\Delta}^2} . \quad (30)$$

In case of Type-II seesaw, only one diagram in the complete high energy theory contributes to the effective low energy neutrino mass operator, as shown in Table 2, and we have

$$\mathcal{A} = i \frac{\Lambda_6}{\mathbb{M}_{\Delta}^2} (Y_{\Delta})_{fg} (\varepsilon_{ac} \varepsilon_{bd} + \varepsilon_{ab} \varepsilon_{cd}) , \quad (31)$$

and comparison with Eq. (14) gives

$$\kappa = - \frac{2 \Lambda_6 Y_{\Delta}}{\mathbb{M}_{\Delta}^2} . \quad (32)$$

Hence finally one gets the neutrino mass to be

$$\mathfrak{m}_{\nu} = - \frac{v^2}{4} \kappa = \frac{v^2}{2} \frac{\Lambda_6 Y_{\Delta}}{\mathbb{M}_{\Delta}^2} , \quad (33)$$

which is the same as the Type-II seesaw relation, as given in Eq. (30).

Just like the right-handed neutrinos in case of Type-I seesaw, the Higgs triplets in Type-II seesaw will decouple step by step at their respective mass scales and the effective theories have to be matched against each other. The decoupling of the right-handed neutrinos only contributes to the effective 5-dimensional neutrino mass operator, while the decoupling of the Higgs triplet also gives a contribution to the SM model Higgs self-coupling because there is a coupling between the SM Higgs doublet and the Higgs triplet given in Eq. (26). The matching condition for the Higgs self-coupling at the threshold is given as

$$\lambda^{\text{EFT}} = \lambda + 2 \frac{|\Lambda_6|^2}{\mathbb{M}_{\Delta}^2} . \quad (34)$$

2.2.3 Type-III seesaw

Type-III seesaw mechanism is mediated by heavy fermion triplets transforming in the adjoint representation of $SU(2)_L$ and has been considered earlier in [39, 40]. Very recently there has been a renewed interest in these type of models. The smallness of neutrino masses usually implies the mass of the heavy particle to be high $\sim 10^{11-15}$ GeV, as shown in Chapter 2.1. However, it is also possible that one or more of the triplets have masses near the TeV scale, making it possible to search for their signatures at the LHC [45, 46, 47, 48, 49]. In such models, the Yukawa couplings need to be small to suppress the neutrino mass, if no fine tuning of the parameters is assumed. Lepton flavor violating decays in the context of Type-III seesaw models have also been considered in [50]. Recently it has also been suggested that the neutral member of the triplet can serve as the dark matter and can be instrumental in generating small neutrino mass radiatively [51].

In the Type-III seesaw, there are right handed fermionic triplet Σ_R added to the SM at the high scale which is singlet under $U(1)_Y$, while transform as a triplet in the adjoint representation of $SU(2)_L$. This triplet can be represented as

$$\Sigma_R = \begin{pmatrix} \Sigma_R^0/\sqrt{2} & \Sigma_R^+ \\ \Sigma_R^- & -\Sigma_R^0/\sqrt{2} \end{pmatrix} \equiv \frac{\Sigma_R^i \sigma^i}{\sqrt{2}}, \quad (35)$$

where $\Sigma_R^\pm = (\Sigma_R^1 \mp i\Sigma_R^2)\sqrt{2}$. For the sake of simplicity of further calculations, we combine Σ_R with its CP conjugate Σ_R^C to construct

$$\Sigma \equiv \Sigma_R + \Sigma_R^C. \quad (36)$$

Clearly, Σ also transforms in the adjoint representation of $SU(2)_L$. Note that though formally $\Sigma = \Sigma^C$, the individual elements of Σ are not all Majorana particles. While the diagonal elements of Σ are indeed Majorana spinors which represent the neutral component of Σ , the off-diagonal elements are charged Dirac spinors.

Introduction of this triplet field will introduce new terms in the Lagrangian. The net Lagrangian is

$$\mathcal{L} = \mathcal{L}_{SM} + \mathcal{L}_\Sigma, \quad (37)$$

where

$$\mathcal{L}_\Sigma = \mathcal{L}_{\Sigma,kin} + \mathcal{L}_{\Sigma,mass} + \mathcal{L}_{\Sigma,Yukawa}. \quad (38)$$

Here,

$$\mathcal{L}_{\Sigma,kin} = \text{Tr}[\bar{\Sigma} i \not{D} \Sigma] , \quad (39)$$

$$\mathcal{L}_{\Sigma,mass} = -\frac{1}{2} \text{Tr}[\bar{\Sigma} M_{\Sigma} \Sigma] , \quad (40)$$

$$\mathcal{L}_{\Sigma,Yukawa} = -\bar{l}_L \sqrt{2} Y_{\Sigma}^{\dagger} \Sigma \tilde{\phi} - \phi^T \varepsilon^T \bar{\Sigma} \sqrt{2} Y_{\Sigma} l_L . \quad (41)$$

Here we have not written the generation indices explicitly. M_{Σ} is the Majorana mass matrix of the heavy fermion triplets and Y_{Σ} is the Yukawa coupling. Since the fermion triplet Σ is in the adjoint representation of $SU(2)_L$, the covariant derivative of Σ is defined as

$$D_{\mu} \Sigma = \partial_{\mu} \Sigma + i g_2 [W_{\mu}, \Sigma] , \quad (42)$$

where g_2 is the $SU(2)_L$ gauge coupling. Unlike Δ , Σ being a singlet under $U(1)_Y$ does not couple to B_{μ} .

The new term \mathcal{L}_{Σ} in the Lagrangian, as shown in Eq. (38), can be expanded as [50]

$$\begin{aligned} \mathcal{L}_{\Sigma} = & \left(\bar{\Psi} i \not{\partial} \Psi + \bar{\Sigma}_R^0 i \not{\partial} \Sigma_R^0 + \text{h.c.} \right) \\ & + g_2 \left(W_{\mu}^+ \bar{\Sigma}_R^0 \gamma^{\mu} P_R \Psi + W_{\mu}^+ \bar{\Sigma}_R^{0C} \gamma^{\mu} P_L \Psi + \text{h.c.} \right) - g_2 W_{\mu}^3 \bar{\Psi} \gamma^{\mu} \Psi \\ & - \bar{\Psi} M_{\Sigma} \Psi - \left(\frac{1}{2} \bar{\Sigma}_R^0 M_{\Sigma} \Sigma_R^{0C} + \text{h.c.} \right) \\ & - \left(\phi^0 \bar{\Sigma}_R^0 Y_{\Sigma} \nu_L + \sqrt{2} \phi^0 \bar{\Psi} Y_{\Sigma} l_L + \phi^+ \bar{\Sigma}_R^0 Y_{\Sigma} l_L - \sqrt{2} \phi^+ \bar{\nu}_L^C Y_{\Sigma}^T \Psi + \text{h.c.} \right) . \end{aligned} \quad (43)$$

Here we have defined the four component Dirac spinor

$$\Psi \equiv \Sigma_R^{+C} + \Sigma_R^{-} , \quad (44)$$

for our convenience, while the neutral component of Σ_R is still in the two component notation. In Eq. (43), the first two lines come from $\mathcal{L}_{\Sigma,kin}$, the third line corresponds to the Majorana mass term in $\mathcal{L}_{\Sigma,mass}$ and the terms in the last line corresponds to the Yukawa coupling terms in $\mathcal{L}_{\Sigma,Yukawa}$, as given in Eqs. (39)–(41). After the electroweak symmetry breaking, the mass matrix for the neutral fields become

$$\mathcal{L} \ni -\frac{1}{2} \begin{pmatrix} \bar{\nu}_L^C & \bar{\Sigma}_R^0 \end{pmatrix} \begin{pmatrix} 0 & m_D \\ m_D^T & M_{\Sigma} \end{pmatrix} \begin{pmatrix} \nu_L \\ \Sigma_R^{0C} \end{pmatrix} + \text{h.c.} , \quad (45)$$

where $m_D = (v/\sqrt{2}) Y_{\Sigma}^T$ is the Dirac mass matrix of the neutral fields. Thus the mass matrix in Eq. (45) looks the same as that obtained in Eq. (10)

and hence for large M_Σ , diagonalization of the mass matrix will produce light active neutrino states via seesaw mechanism, as obtained in Sec 2.2.1. The seesaw achieved here with the help of the neutral component of the fermionic triplet is known as the Type-III seesaw mechanism. Eq. (45) also implies that there will be a mixing between the light and the heavy neutral states, however the mixing angle will be $\mathcal{O}(m_D/M_\Sigma)$ and hence very small for large M_Σ .

Since the heavy fermion triplets added to the SM at the high scale have charged components also, they will modify the masses of the charged leptons belonging to the SM, in addition to the generation of the small active neutrino masses. With the addition of the triplet fields, the mass term of the charged lepton sector after electroweak symmetry breaking becomes

$$\begin{aligned} \mathcal{L} \ni & - (\bar{l}_R \quad \bar{\Psi}_R) \begin{pmatrix} m_L & 0 \\ \sqrt{2}m_D^T & M_\Sigma \end{pmatrix} \begin{pmatrix} l_L \\ \Psi_L \end{pmatrix} \\ & - (\bar{l}_L \quad \bar{\Psi}_L) \begin{pmatrix} m_L & \sqrt{2}m_D^* \\ 0 & M_\Sigma \end{pmatrix} \begin{pmatrix} l_R \\ \Psi_R \end{pmatrix} \\ = & - (\bar{l}_R \quad \bar{\Psi}_R) \mathcal{M}_c \begin{pmatrix} l_L \\ \Psi_L \end{pmatrix} - (\bar{l}_L \quad \bar{\Psi}_L) \mathcal{M}_c^\dagger \begin{pmatrix} l_R \\ \Psi_R \end{pmatrix}, \end{aligned} \quad (46)$$

where m_L is the Dirac mass matrix of the SM charged leptons and

$$\mathcal{M}_c \equiv \begin{pmatrix} m_L & 0 \\ \sqrt{2}m_D^T & M_\Sigma \end{pmatrix} \quad (47)$$

denotes the complete mass matrix for the charged leptons. Eq. (47) shows that the inclusion of the charged fermions as components of the heavy triplets does not change the masses of the charged leptons of the SM upto the order $\mathcal{O}((m_D, m_L)/M_\Sigma)$. However, there will be mixing between the states l_L - Ψ_L and l_R - Ψ_R , but the mixing angle is small in the $m_D, m_L \ll M_\Sigma$ limit. The correction to the charged lepton masses due to the charged components of the triplet fermion in $\mathcal{O}([(m_D, m_L)/M_\Sigma]^2)$ can be calculated easily from [47].

As can be seen from the Table 2, the diagrams in the complete Type-III seesaw theory giving rise to the effective operators in the low energy limit are very similar to the case of Type-I seesaw. Here the amplitudes $\mathcal{A}_{(a)}$ and $\mathcal{A}_{(b)}$ are given by

$$\mathcal{A}_{(a)} = i\mu^\epsilon (Y_\Sigma^T M_\Sigma^{-1} Y_\Sigma)_{fg} [(\varepsilon^T \sigma^i)_{ab} (\varepsilon^T \sigma^i)_{cd}] P_L, \quad (48)$$

$$\mathcal{A}_{(b)} = i\mu^\epsilon (Y_\Sigma^T M_\Sigma^{-1} Y_\Sigma)_{fg} [(\varepsilon^T \sigma^i)_{db} (\varepsilon^T \sigma^i)_{ca}] P_L. \quad (49)$$

Using Eq. (15) one finally gets

$$\mathcal{A}_{(a)} + \mathcal{A}_{(b)} = -i\mu^\epsilon (Y_\Sigma^T M_\Sigma^{-1} Y_\Sigma)_{fg} (\varepsilon_{ab} \varepsilon_{cd} + \varepsilon_{ac} \varepsilon_{bd}) P_L, \quad (50)$$

which gives

$$\kappa = 2Y_{\Sigma}^T \mathbb{M}_{\Sigma}^{-1} Y_{\Sigma} . \quad (51)$$

From Eqs. (14) and (51) one gets the neutrino mass after spontaneous symmetry breaking to be

$$m_{\nu} = -\frac{v^2}{2} Y_{\Sigma}^T \mathbb{M}_{\Sigma}^{-1} Y_{\Sigma} \quad (52)$$

which is the Type-III seesaw relation. Here, v denotes the vacuum expectation value of the Higgs field.

2.2.4 Inverse seesaw

Apart from the three types of seesaws described in Sec. 2.2.1–2.2.3, there is another well-known scenario known as the Inverse Seesaw. In the Inverse Seesaw scenario [25], additional SM gauge singlets are introduced together with a small Majorana mass insertion through the additional right handed heavy singlets which explicitly breaks the lepton number. The minimal version of this Inverse Seesaw scenario requires the addition of two right-handed neutrinos N_R^f and two left-handed SM gauge singlets S_L^f , where $f \in \{1, 2\}$ is the generation index [55, 56]. We construct the field N^f and S^f as

$$N^f = N_R^f + N_R^{Cf} , \quad (53)$$

$$S^f = S_L^f + S_L^{Cf} , \quad (54)$$

and then the Lagrangian for the theory will be given by

$$\mathcal{L} = \mathcal{L}_{\text{SM}} + \mathcal{L}_{IS} , \quad (55)$$

where \mathcal{L}_{IS} is the contribution from the fields added to the SM to produce the Inverse Seesaw and is given as

$$\mathcal{L}_{IS} = \mathcal{L}_{IS,kin} + \mathcal{L}_{IS,Yukawa} + \mathcal{L}_{IS,mass} , \quad (56)$$

where

$$\mathcal{L}_{IS,kin} = \frac{1}{2} \overline{N}^f (i\partial)_{fg} N^g + \frac{1}{2} \overline{S}^f (i\partial)_{fg} S^g , \quad (57)$$

$$\mathcal{L}_{IS,Yukawa} = -\overline{N}^f (Y_N)_{fg} \tilde{\phi}^\dagger l_L^g + \text{h.c.} , \quad (58)$$

$$\mathcal{L}_{IS,mass} = -\overline{S}^f (\mathbb{M}_R)_{fg} N^g - \frac{1}{2} \overline{S}^f \mu_{fg} S^{Cg} + \text{h.c.} , \quad (59)$$

where the generation indices g, f are written down explicitly. Here μ is a complex symmetric 2×2 matrix and Y_N and \mathbb{M}_R are arbitrary 3×2 and 2×2

matrices, respectively. Without loss of generality, one can always redefine the extra singlet fields and work in a basis where μ is real and diagonal. After the electroweak symmetry breaking, the Lagrangian giving rise to the 7×7 mass matrix for the neutral fields ν_L^f , N^f and S^f can be expressed as

$$\mathcal{L} \ni \begin{pmatrix} \bar{\nu}_L & \overline{N_R^C} & \overline{S_L} \end{pmatrix} \begin{pmatrix} 0 & \mathfrak{m}_D & 0 \\ \mathfrak{m}_D^T & 0 & \mathbb{M}_R^T \\ 0 & \mathbb{M}_R & \mu \end{pmatrix} \begin{pmatrix} \nu_L^C \\ N_R \\ S_L^C \end{pmatrix} + \text{h.c.} , \quad (60)$$

where the Dirac mass matrix is defined as $\mathfrak{m}_D = (v/\sqrt{2})Y_N^T$. It should be noted that \mathbb{M}_R and μ being the mass terms of the SM singlet fields do not depend on the scale of the $SU(2)_L$ symmetry breaking.

At the leading order in $\mathfrak{m}_D \mathbb{M}_R^{-1}$, the active light neutrino mass matrix is given by

$$\mathfrak{m}_\nu \approx \mathfrak{m}_D \mathbb{M}_R^{-1} \mu (\mathbb{M}_R^T)^{-1} \mathfrak{m}_D^T \equiv F \mu F^T , \quad (61)$$

where $F \equiv \mathfrak{m}_D \mathbb{M}_R^{-1}$. In this case, for $\mu \sim 10^3$ eV, the light neutrino mass can be $\mathfrak{m}_\nu \sim 0.01$ eV if $F \sim 0.3 \times 10^{-2}$. Thus for the Yukawa couplings $Y_N \sim 0.1 - 1$, the heavy singlets can be in the mass range $10^4 - 10^5$ GeV and the seesaw scales can be lowered by orders of magnitudes compared to the Type-I seesaw.

3 RG evolution of neutrino masses and mixing in effective theories

Now we consider the radiative corrections to the masses, mixing parameters and couplings in the effective low energy theory of neutrino masses. As can be understood from the discussions in Sec. 2, there is a unique dimension-5 operator given in Eq. (4), that gives rise to the light neutrino masses after spontaneous symmetry breaking and hence is the same for all three types of seesaws. Thus the RG evolution equations will depend solely on the underlying theory. Throughout this paper, we consider the SM as the low energy effective theory. However, to discuss the RG evolution in the effective theory, we will also consider the Minimal Supersymmetric Standard Model (MSSM) and discuss the effect of $\tan\beta$.

In order to evaluate the β -functions, one need to compute the renormalization constants for wavefunctions, couplings, etc. For this purpose any regularization scheme can be chosen from dimensional regularization, Pauli-Villars method, Ultra-Violet cutoff etc. and then the scheme for renormalization has to be fixed [60]. For the purpose of calculation of the renormalization

	SM
$16\pi^2\beta_\kappa$	$-\frac{3}{2}\left(Y_e^\dagger Y_e\right)^T \kappa - \frac{3}{2}\kappa\left(Y_e^\dagger Y_e\right) + (2T + \lambda - 3g_2^2)\kappa$
$16\pi^2\beta_{Y_e}$	$Y_e\left(\frac{3}{2}Y_e^\dagger Y_e + T - \frac{9}{4}g_1^2 - \frac{9}{4}g_2^2\right)$
$16\pi^2\beta_{Y_u}$	$Y_u\left(\frac{3}{2}Y_u^\dagger Y_u - \frac{3}{2}Y_d^\dagger Y_d + T - \frac{17}{20}g_1^2 - \frac{9}{4}g_2^2 - 8g_3^2\right)$
$16\pi^2\beta_{Y_d}$	$Y_d\left(\frac{3}{2}Y_d^\dagger Y_d - \frac{3}{2}Y_u^\dagger Y_u + T - \frac{1}{4}g_1^2 - \frac{9}{4}g_2^2 - 8g_3^2\right)$
$16\pi^2\beta_\lambda$	$6\lambda^2 - 3\lambda\left(\frac{3}{5}g_1^2 + 3g_2^2\right) + 3g_2^4 + \frac{3}{2}\left(\frac{3}{5}g_1^2 + g_2^2\right)^2 + 4\lambda T - 8T'$
$16\pi^2g_i$	$b_i g_i^3 \text{ (} b_1 = \frac{41}{10}, b_2 = -\frac{19}{6}, b_3 = -7 \text{)}$
T	$\text{Tr}\left[Y_e^\dagger Y_e + 3Y_u^\dagger Y_u + 3Y_d^\dagger Y_d\right]$
T'	$\text{Tr}[Y_e^\dagger Y_e Y_e^\dagger Y_e + 3Y_u^\dagger Y_u Y_u^\dagger Y_u + 3Y_d^\dagger Y_d Y_d^\dagger Y_d]$
	MSSM
$16\pi^2\beta_\kappa$	$\left(Y_e^\dagger Y_e\right)^T \kappa + \kappa\left(Y_e^\dagger Y_e\right) + (2T_1 - \frac{6}{5}g_1^2 - 6g_2^2)\kappa$
$16\pi^2\beta_{Y_e}$	$Y_e\left(3Y_e^\dagger Y_e + T_2 - \frac{9}{5}g_1^2 - 3g_2^2\right)$
$16\pi^2\beta_{Y_u}$	$Y_u\left(3Y_u^\dagger Y_u + Y_d^\dagger Y_d + T_1 - \frac{13}{15}g_1^2 - 3g_2^2 - \frac{16}{3}g_3^2\right)$
$16\pi^2\beta_{Y_d}$	$Y_d\left(3Y_d^\dagger Y_d + Y_u^\dagger Y_u + T_2 - \frac{7}{15}g_1^2 - 3g_2^2 - \frac{16}{3}g_3^2\right)$
$16\pi^2g_i$	$b_i g_i^3 \text{ (} b_1 = \frac{33}{5}, b_2 = 1, b_3 = -3 \text{)}$
T_1	$\text{Tr}\left[3Y_u^\dagger Y_u\right]$
T_2	$\text{Tr}\left[Y_e^\dagger Y_e + 3Y_d^\dagger Y_d\right]$

Table 3: Evolution equations for the Yukawa couplings Y_e , Y_u , Y_d , gauge couplings g_1 , g_2 , g_3 , Higgs self-coupling λ (SM only) and the effective neutrino mass operator κ in the SM and the MSSM [36, 58, 68, 104]. Here we have used the GUT charge renormalization and hence $g_1 \equiv g_1^{\text{Unified}} = \sqrt{5/3} g_1^{\text{SM}}$. This convention has been followed through out this review. Here $\beta_X \equiv \mu(dX/d\mu)$.

constants, the gauge also has to be fixed. However, the final β -functions must be independent of the particular regularization as well as the renormalization scheme used for the calculations, and also of the gauge choice. β -functions can be determined from the renormalization constants using the functional differentiation method, as described in [36, 70]. The running equations for the Yukawa couplings, gauge couplings, Higgs self-coupling (in case of the SM only) and the effective neutrino mass operator in the SM and the MSSM are given in Table 3. Finally, after electroweak symmetry breaking, the light neutrino mass matrix is given by

$$m_\nu = -\frac{v^2}{4}\kappa, \quad (62)$$

and thus will have the same evolution as κ . To simplify later discussions, the evolution equation for \mathfrak{m}_ν can be expressed as

$$16\pi^2\beta_{\mathfrak{m}_\nu} = P^T\mathfrak{m}_\nu + \mathfrak{m}_\nu P + \alpha_\nu\mathfrak{m}_\nu \quad (63)$$

where $\beta_X \equiv dX/d\ln(\mu/\text{GeV})$ and

$$P = C_e Y_e^\dagger Y_e. \quad (64)$$

Here the values of C_e and α_ν depend on the underlying theory, and can be read off from Table 3 when the theory is the SM or the MSSM. Without any loss of generality we can always choose the charged lepton Yukawa matrix Y_e as well as the quark Yukawa matrices Y_u and Y_d to be diagonal at the high scale. Then from the RG equations in Table 3 we get that they will remain diagonal at all energy scales, and so will P . Thus the evolution of the components of κ , and hence of \mathfrak{m}_ν , will be proportional to themselves.

3.1 Evolution equations for neutrino parameters from matrix equations

At any energy scale μ , the neutrino mass matrix \mathfrak{m}_ν and the charged lepton Yukawa $Y_e^\dagger Y_e$ can be diagonalized by unitary transformations via [104]

$$U_\nu(\mu)^T \mathfrak{m}_\nu(\mu) U_\nu(\mu) = \text{Diag}(m_1(\mu), m_2(\mu), m_3(\mu)), \quad (65)$$

$$U_e(\mu)^\dagger Y_e^\dagger Y_e(\mu) U_e(\mu) = \text{Diag}(y_e^2(\mu), y_\mu^2(\mu), y_\tau^2(\mu)), \quad (66)$$

where U_ν and U_e are unitary matrices and the neutrino mixing matrix will then be given by

$$U_{\text{PMNS}}(\mu) = U_e^\dagger(\mu) U_\nu(\mu). \quad (67)$$

Since in the effective theory $Y_e^\dagger Y_e$ remains diagonal at all energies, as discussed in the previous section, $U_e(\mu) = \mathbb{1}$ in Eq. (66) and from Eq. (67) one has $U_{\text{PMNS}}(\mu) = U_\nu(\mu)$. Thus the RG evolution of $U_{\text{PMNS}}(\mu)$ will be governed by the running of \mathfrak{m}_ν only. The evolution of the mixing matrix U_ν will be given by [61]

$$\frac{dU_\nu}{dt} = U_\nu T, \quad (68)$$

where $t \equiv \ln(\mu/\text{GeV})/16\pi^2$ and T is an anti-Hermitian matrix defined as [61]

$$16\pi^2 \text{Re}T_{ij} = \begin{cases} 0 & (i = j), \\ -\frac{m_i + m_j}{m_i - m_j} \text{Re}P'_{ij} & (i \neq j), \end{cases} \quad (69)$$

$$16\pi^2 \text{Im}T_{ij} = -\frac{m_i - m_j}{m_i + m_j} \text{Im}P'_{ij}, \quad (70)$$

where $P' = U_\nu^\dagger P U_\nu$, with P defined by Eqs. (63)-(64). In order to obtain the RG evolution equations for the mixing angles and the phases, one has to solve the system of nine coupled equations in the parameters $\xi_k = \{\theta_{12}, \theta_{23}, \theta_{13}, \delta, \phi_1, \phi_2, \delta_e, \delta_\mu, \delta_\tau\}$, obtained from Eq. (68) using the definition of T as given in Eqs. (69)-(70) and then using the parametrization of U_{PMNS} as given in Eqs. (1)-(3).

3.1.1 RG evolution of the mixing angles and phases

The RG evolution equations for the mixing angles can be written in general as [36, 104, 61]

$$\dot{X} = \frac{D_X}{\theta_{13}} + A_X + \mathcal{O}(\theta_{13}) , \quad (71)$$

where $X \in \{\theta_{12}, \theta_{23}, \theta_{13}, \delta, \phi_1, \phi_2\}$. The differentiation is performed w.r.t. $t \equiv \ln(\mu/\text{GeV})/16\pi^2$. It can be seen that the quantities $D_X = 0$ for all X except D_{13} . Evolution of the mixing angles are given by

$$A_{12} = -\frac{C y_\tau^2}{2} \sin 2\theta_{12} s_{23}^2 \frac{|m_1 e^{2i\phi_1} + m_2 e^{2i\phi_2}|^2}{\Delta m_\odot^2} , \quad (72)$$

$$A_{23} = -\frac{C y_\tau^2}{2} \sin 2\theta_{23} \left[c_{12}^2 \frac{|m_2 e^{2i\phi_2} + m_3|^2}{\Delta m_{\text{atm}}^2} + s_{12}^2 \frac{|m_1 e^{2i\phi_1} + m_3|^2}{\Delta m_{\text{atm}}^2 (1 + \zeta)} \right] , \quad (73)$$

$$A_{13} = \frac{C y_\tau^2}{2} \sin 2\theta_{12} \sin 2\theta_{23} \frac{m_3}{\Delta m_{\text{atm}}^2 (1 + \zeta)} \times [m_1 \cos(2\phi_1 - \delta) - (1 + \zeta)m_2 \cos(2\phi_2 - \delta) - \zeta m_3] , \quad (74)$$

where $\zeta = \Delta m_\odot^2 / \Delta m_{\text{atm}}^2$ and $c_{ij} = \cos \theta_{ij}$, $s_{ij} = \sin \theta_{ij}$. As can be seen from Table 3, $C = C_e = -3/2$ for the SM and $C = C_e = 1$ for the MSSM. Here y_e^2 and y_μ^2 are neglected compared to y_τ^2 . The quantities governing the evolution of the Dirac CP phase δ are given as

$$A_\delta = 2C y_\tau^2 \left\{ \frac{m_1 m_2}{\Delta m_\odot^2} s_{23}^2 \sin(2\phi_1 - 2\phi_2) + \frac{m_3}{\Delta m_{\text{atm}}^2 (1 + \zeta)} [c_{23}^2 (m_1 c_{12}^2 \sin(2\delta - 2\phi_1) + m_2 (1 + \zeta) s_{12}^2 \sin(2\delta - 2\phi_2)) + \cos 2\theta_{23} (m_1 s_{12}^2 \sin 2\phi_1 + m_2 (1 + \zeta) c_{12}^2 \sin 2\phi_2)] \right\} , \quad (75)$$

$$D_\delta = \frac{C y_\tau^2}{2} \sin 2\theta_{12} \sin 2\theta_{23} \frac{m_3}{\Delta m_{\text{atm}}^2 (1 + \zeta)} \times [m_1 \sin(2\phi_1 - \delta) - (1 + \zeta)m_2 \sin(2\phi_2 - \delta) + \zeta m_3 \sin \delta] , \quad (76)$$

while those for the Majorana phases ϕ_1, ϕ_2 are

$$A_{\phi_1} = 2Cy_\tau^2 \left\{ m_3 \cos 2\theta_{23} \frac{m_1 s_{12}^2 \sin 2\phi_1 + (1 + \zeta) m_2 c_{12}^2 \sin 2\phi_2}{\Delta m_{\text{atm}}^2 (1 + \zeta)} + \frac{m_1 m_2 c_{12}^2 s_{23}^2 \sin (2\phi_1 - 2\phi_2)}{\Delta m_\odot^2} \right\}, \quad (77)$$

$$A_{\phi_2} = 2Cy_\tau^2 \left\{ m_3 \cos 2\theta_{23} \frac{m_1 s_{12}^2 \sin 2\phi_1 + (1 + \zeta) m_2 c_{12}^2 \sin 2\phi_2}{\Delta m_{\text{atm}}^2 (1 + \zeta)} + \frac{m_1 m_2 s_{12}^2 s_{23}^2 \sin (2\phi_1 - 2\phi_2)}{\Delta m_\odot^2} \right\}. \quad (78)$$

3.1.2 RG evolution of the light neutrino masses

Using the definition of U_ν in Eq. (65) and T in Eq. (68), the RG evolution of the light neutrino masses is obtained from Eq. (63) to be

$$\dot{m}_i = (\text{Re}\alpha_\nu + 2\text{Re}P'_{ii}) m_i, \quad (79)$$

where no summation over the repeated index ‘ i ’ is to be taken. The evolution of the individual masses in terms of the mixing parameters becomes

$$\dot{m}_1 = [\alpha_\nu + Cy_\tau^2 (2s_{12}^2 s_{23}^2 + G_1)] m_1, \quad (80)$$

$$\dot{m}_2 = [\alpha_\nu + Cy_\tau^2 (2c_{12}^2 s_{23}^2 + G_2)] m_2, \quad (81)$$

$$\dot{m}_3 = [\alpha_\nu + 2Cy_\tau^2 c_{13}^2 c_{23}^2] m_3, \quad (82)$$

where

$$G_1 = -s_{13} \sin 2\theta_{12} \sin 2\theta_{23} \cos \delta + 2s_{13}^2 c_{12}^2 c_{23}^2, \quad (83)$$

$$G_2 = s_{13} \sin 2\theta_{12} \sin 2\theta_{23} \cos \delta + 2s_{13}^2 s_{12}^2 c_{23}^2. \quad (84)$$

From the Eqs. (80)–(82) it can be seen that the evolution of a particular mass eigenvalue is proportional to itself upto $\mathcal{O}(\theta_{13}^0)$ and thus if some m_i is zero to start with along with $\theta_{13} = 0$, it will remain so. However, it is the characteristic of the 1-loop RG evolution only, and breaks down when the 2-loop contributions are taken into account [59].

To study the RG evolution of the neutrino masses and the mixing parameters in the effective theory, we consider μ_0 to be the high energy scale below which the effective theory gives the correct description of the light neutrino

masses, which we also take to be the mass of the lightest heavy particle responsible for the seesaw mechanism. Then at any energy scale μ , the value of the mixing angles can be expressed as

$$\theta_{ij} = \theta_{ij}^0 + \int_{t_0}^t A_{ij}(t') dt' + \mathcal{O}(\theta_{13}) \quad (85)$$

$$\approx \theta_{ij}^0 + k_{ij} \Delta_\tau + \mathcal{O}(\Delta_\tau \theta_{13}, \Delta_\tau^2), \quad (86)$$

where $t_0 \equiv \ln(\mu_0/\text{GeV})/16\pi^2$ and θ_{ij}^0 is the value of the angle at the high energy μ_0 . In Eq. (86), Δ_τ is defined as

$$\Delta_\tau^{\text{SM}} \equiv -\frac{1}{32\pi^2} \left(\frac{g_2 m_\tau}{M_W} \right)^2 \ln \left(\frac{\mu_0}{\mu} \right) \quad (87)$$

in the SM, where g_2 is the $\text{SU}(2)_L$ gauge coupling, whereas m_τ and M_W are the τ lepton and W boson masses respectively. In the MSSM,

$$\Delta_\tau^{\text{MSSM}} \equiv -\frac{1}{32\pi^2} \left(\frac{g_2 m_\tau}{M_W} \right)^2 (1 + \tan^2 \beta) \ln \left(\frac{\mu_0}{\mu} \right). \quad (88)$$

Numerically, one has $\Delta_\tau^{\text{SM}} \approx -1.4 \times 10^{-5}$ when $\mu_0 = 10^{12}$ GeV and $\mu = 10^2$ GeV. For MSSM, $\Delta_\tau^{\text{MSSM}} \approx -1.3 \times 10^{-5} (1 + \tan^2 \beta)$, where $\mu = 10^3$ GeV and $\tan \beta$ can take values upto ~ 50 . Hence in both the cases one can treat these quantities as small parameters. The quantities k_{ij} can then be written from Eqs. (72)-(74) as

$$k_{12} = -\frac{C}{2} \sin 2\theta_{12} s_{23}^2 \frac{|m_1 e^{2i\phi_1} + m_2 e^{2i\phi_2}|^2}{\Delta m_{\odot}^2}, \quad (89)$$

$$k_{23} = -\frac{C}{2} \sin 2\theta_{23} \left[c_{12}^2 \frac{|m_2 e^{2i\phi_2} + m_3|^2}{\Delta m_{\text{atm}}^2} + s_{12}^2 \frac{|m_1 e^{2i\phi_1} + m_3|^2}{\Delta m_{\text{atm}}^2 (1 + \zeta)} \right], \quad (90)$$

$$k_{13} = \frac{C}{2} \sin 2\theta_{12} \sin 2\theta_{23} \frac{m_3}{\Delta m_{\text{atm}}^2 (1 + \zeta)} \times [m_1 \cos(2\phi_1 - \delta) - (1 + \zeta)m_2 \cos(2\phi_2 - \delta) - \zeta m_3]. \quad (91)$$

The same results are obtained in [63, 64, 65] following a slightly different approach given in [66, 67, 68]. Similar integrated evolution equations can be written for the Majorana phases as

$$\phi_i = \phi_i^0 + k_{\phi_i} \Delta_\tau + \mathcal{O}(\Delta_\tau \theta_{13}, \Delta_\tau^2), \quad (92)$$

where ϕ_i^0 is the value of ϕ_i at μ_0 and k_{ϕ_i} can be read off directly from Eqs. (77)-(78). However, the running of the Dirac CP phase δ has to be considered

carefully, since D_δ is non-zero and θ_{13} is allowed to take small values including zero. This issue will be discussed in detail in Sec 3.1.3.

From k_{12} in Eq. (89) it can be seen that the solar mixing angle θ_{12} generically has the strongest RG effects among the mixing angles. The reason for this is the smallness of the Δm_\odot^2 associated with it, in particular compared to Δm_{atm}^2 , which leads to an enhanced running for quasi-degenerate neutrinos and for the case of an inverted mass hierarchy. The running is maximum for $|\phi_1 - \phi_2| = 0$, and minimum for $|\phi_1 - \phi_2| = \pi/2$. As it is clear from Eq. (89), the direction of the running depends solely on $C\Delta_\tau$. Hence for evolution from a high to a low energy scale, θ_{12} always increases in the MSSM, and decreases in the SM. From Eq. (90) it is evident that the direction of the θ_{23} evolution depends on $C\Delta_\tau$ as well as on the hierarchy. However, the running of θ_{13} depends on specific combinations of the CP phases, as shown in Eq. (91). If the symmetry $\theta_{13} = 0$ is implemented at the high scale μ_0 [62], which is the case for many neutrino mass models, the maximum θ_{13} value can be achieved with the choice

$$2\phi_1 - \delta_0 = 0, \quad |2\phi_2 - \delta_0| = \pi, \quad (93)$$

δ_0 being the Dirac CP phase at μ_0 and finally

$$\theta_{13}^{\text{max}} \leq \frac{|C|\Delta_\tau}{2} \sin 2\theta_{12} \sin 2\theta_{23} \frac{m_3}{|\Delta m_{31}^2|} [m_1 + (1 + \zeta)m_2 + |\zeta|m_3]. \quad (94)$$

To consider the running of the Majorana phases, one gets combining Eqs. (77)-(78) and Eq. (92)

$$k_{\phi_1} - k_{\phi_2} = 2C \cos 2\theta_{12} s_{23}^2 \frac{m_1 m_2}{\Delta m_\odot^2} \sin(2\phi_1 - 2\phi_2), \quad (95)$$

which shows that if $(\phi_1 - \phi_2) = 0$ at some scale, it will remain so at all energy scales, upto $\mathcal{O}(\theta_{13}^0)$. Moreover, if $(\phi_1 - \phi_2)$ is small at some scale so that we can write $\sin(2\phi_1 - 2\phi_2) \approx 2(\phi_1 - \phi_2)$, the running of $(\phi_1 - \phi_2)$ is proportional to itself. However, the $\mathcal{O}(\theta_{13})$ term may become important for large $\tan \beta$ values in case of the MSSM and then it will be possible to generate $(\phi_1 - \phi_2)$ radiatively.

The running of the mass eigenvalues is significant even in the SM or for strongly hierarchical neutrino masses due to the factor α_ν in the RG evolution equations given in Eqs. (80)-(82). As can be seen explicitly, the evolutions are not directly dependent on the Majorana phases, and the dependence on the Dirac CP phase δ is proportional to $\sin \theta_{13}$. Moreover, apart from the MSSM with very large $\tan \beta$ or at very high energy values, the running of the mass eigenvalues is solely controlled by the term proportional to α_ν , and there will be very small dependence on the mixing parameters. Thus in such

cases, the running is given by a common scaling of the mass eigenvalues [61, 68] and can be given by

$$m_i \approx m_i^0 \exp \left[\int_{t_0}^t \alpha_\nu(t') dt' \right]. \quad (96)$$

Some generic features of the RG evolution of the light neutrino masses and the mixing parameters in the effective theory have been studied extensively in literature [61, 68, 69, 70, 58, 71]. These effects can have interesting consequences such as the generation of large mixing angles [72, 73, 74, 75, 76, 77], small mass splittings for degenerate neutrinos [78, 79, 80, 81, 82, 83, 84, 85, 86, 87], or radiative generation of θ_{13} starting from a zero value at the high scale [62, 88, 89, 90]. Some specific features of the RG evolution, like the stability of mixing angles and masses [66, 91, 92, 93, 94], possible occurrence of fixed points [95, 96, 97] have also been studied. RG induced deviations from various high scale symmetries like tri-bimaximal mixing scenario [64, 65, 98] or quark-lepton complementarity [63, 65, 100, 101, 102] and correlations with low scale observables have also been explored in detail.

3.1.3 A subtlety at $\theta_{13} = 0$

As mentioned already, Eq. (75) clearly suggests that A_δ and hence δ diverges for $\theta_{13} \rightarrow 0$. This problem is overcome by requiring that $D_\delta = 0$ at $\theta_{13} = 0$, which gives the following condition on δ at $\theta_{13} = 0$ [61]:

$$\cot \delta = \frac{m_1 \cos 2\phi_1 - (1 + \zeta)m_2 \cos 2\phi_2 - \zeta m_3}{m_1 \sin 2\phi_1 - (1 + \zeta)m_2 \sin 2\phi_2}. \quad (97)$$

The above prescription works for the calculation of evolution when one starts with vanishing θ_{13} . However on the face of it, it seems to imply that the CP phase δ , which does not have any physical meaning at the point $\theta_{13} = 0$, should attain a particular value depending on the masses and Majorana phases, as given in Eq. (97). Moreover, getting the required value of δ precisely when $\theta_{13} = 0$ would seem to need fine tuning when one starts from some non-zero θ_{13} , unless this value of δ is a natural limit of the RG evolution when $\theta_{13} \rightarrow 0$. The problem also propagates to the evolution of θ_{13} , since A_{13} in Eq. (74) depends in turn on δ . The evolution of all the other parameters, viz. m_i , θ_{12}, θ_{23} and ϕ_i is independent of δ upto $\mathcal{O}(\theta_{13}^0)$, and hence will have continuous, non-singular evolution even at $\theta_{13} = 0$. This apparent singularity in δ has been explored in [62] by analyzing the evolution of the complex quantity \mathcal{U}_{e3} , which stays continuous throughout the RG evolution and shows that a fine tuning is indeed required, but that is to ensure that

θ_{13} exactly vanishes. However, if the parameters happen to be tuned such that θ_{13} vanishes exactly, then the limiting value of δ as $\theta_{13} \rightarrow 0$ is always the one given by the prescription mentioned in Eq. (97).

Even after understanding the origin of the apparent singularity in the evolution of δ and hence of θ_{13} , a necessity still remains to have a clear evolution of parameters that reflect the continuous nature of the evolution of elements of the neutrino mixing matrix U_{PMNS} . This can be achieved by choosing the basis as $\mathcal{P}_J = \{m_i, \theta_{12}, \theta_{23}, \theta_{13}^2, \phi_i, J_{\text{CP}}, J'_{\text{CP}}\}$ where the quantities $J_{\text{CP}}, J'_{\text{CP}}$ are defined as

$$J_{\text{CP}} = \frac{1}{2} s_{12} c_{12} s_{23} c_{23} s_{13} c_{13}^2 \sin \delta, \quad (98)$$

$$J'_{\text{CP}} = \frac{1}{2} s_{12} c_{12} s_{23} c_{23} s_{13} c_{13}^2 \cos \delta, \quad (99)$$

instead of the conventional basis $\mathcal{P}_\delta \equiv \{m_i, \theta_{12}, \theta_{23}, \theta_{13}, \phi_i, \delta\}$. From Eqs. (98) and (99) it is seen that $J_{\text{CP}}, J'_{\text{CP}} \rightarrow 0$ as $\theta_{13} \rightarrow 0$ and thus are well-defined. The RG evolution equations for J_{CP} and J'_{CP} are given as

$$\dot{J}_{\text{CP}} = A_J + \mathcal{O}(\theta_{13}), \quad (100)$$

$$\dot{J}'_{\text{CP}} = A'_J + \mathcal{O}(\theta_{13}), \quad (101)$$

with

$$A_J = Cy_\tau^2 s_{12}^2 c_{12}^2 s_{23}^2 c_{23}^2 \frac{m_3 [m_1 \sin 2\phi_1 - (1 + \zeta)m_2 \sin 2\phi_2]}{\Delta m_{\text{atm}}^2 (1 + \zeta)}, \quad (102)$$

$$A'_J = Cy_\tau^2 s_{12}^2 c_{12}^2 s_{23}^2 c_{23}^2 \frac{m_3 [m_1 \cos 2\phi_1 - (1 + \zeta)m_2 \cos 2\phi_2 - \zeta m_3]}{\Delta m_{\text{atm}}^2 (1 + \zeta)}. \quad (103)$$

In the new basis \mathcal{P}_J , the RG evolution for θ_{13}^2 is considered instead of θ_{13} , as is traditionally done. This quantity turns out to have a nonsingular behavior at $\theta_{13} = 0$. Moreover, since $\theta_{13} \geq 0$ by convention, the complete information about θ_{13} lies within θ_{13}^2 . Also, the possible “sign problem”² of θ_{13} is avoided. In terms of the new parameters J_{CP} and J'_{CP} , the RG evolution

²Usually the convention used in defining the elements of U_{PMNS} is to take the angles θ_{ij} to lie in the first quadrant. \mathcal{U}_{e3} can then take both positive or negative values depending on the choice of the CP phase δ . In the formulation of Eq. (74) the sign of A_{13} can be such that θ_{13} can assume negative values during the course of evolution and in such situations one will have to talk about the evolution of $|\theta_{13}|$. Our formulation in terms of θ_{13}^2 , as shown in Eq. (104), naturally avoids this problem.

equations for θ_{13}^2 becomes

$$\dot{\theta}_{13}^2 = A_{13}^{sq} + \mathcal{O}(\theta_{13}^2), \quad (104)$$

$$A_{13}^{sq} = 8C y_\tau^2 \frac{m_3}{\Delta m_{\text{atm}}^2 (1 + \zeta)} \left\{ J_{\text{CP}} [m_1 \sin 2\phi_1 - (1 + \zeta)m_2 \sin 2\phi_2] \right. \\ \left. + J'_{\text{CP}} [m_1 \cos 2\phi_1 - (1 + \zeta)m_2 \cos 2\phi_2 - \zeta m_3] \right\}. \quad (105)$$

Thus the evolution equations in basis \mathcal{P}_J are all non-singular and continuous at every point. In particular, even when δ shows a discontinuity, J_{CP} as well as J'_{CP} change in a continuous manner. This very fact can be used to write down the approximated integrated evolution equations for J_{CP} , J'_{CP} as

$$J_{\text{CP}} = J_{\text{CP}}^0 + k_{J_{\text{CP}}} \Delta\tau + \mathcal{O}(\Delta\tau \theta_{13}, \Delta\tau^2), \quad (106)$$

$$J'_{\text{CP}} = J_{\text{CP}}'^0 + k_{J'_{\text{CP}}} \Delta\tau + \mathcal{O}(\Delta\tau \theta_{13}, \Delta\tau^2), \quad (107)$$

where J_{CP}^0 , $J_{\text{CP}}'^0$ are the initial values at μ_0 and $k_{J_{\text{CP}}}$, $k_{J'_{\text{CP}}}$ can be obtained from Eqs.(102)-(103). From the J_{CP} , J'_{CP} values, the Dirac CP phase δ can be determined unambiguously at any energy scale.

4 RG evolution of neutrino masses and mixing in high energy seesaw models

As discussed in Sec 3, the RG evolution of the neutrino masses and mixing parameters in the low energy effective theory is the same for all three types of seesaw scenarios and depends only on whether the low energy effective theory is the SM or the MSSM. However, this is not true in the high energy theory, when the heavy particles responsible for seesaw remain coupled to the theory. Hence in this case the RG evolution of the different neutrino parameters should also depend on the interaction of these heavy particles with other fields. The importance of including the effects from energy ranges above and between these mass thresholds when analyzing RG effects in GUT models has been pointed out in [72, 80, 81, 90, 103, 57, 104, 105, 106]. These effects are typically at least as important as the RG evolution effects from below the thresholds since the relevant couplings may also be of order one.

The diagrams contributing to the renormalization constants of the different quantities at high energy are shown in [36], [42] and [107] in case of Type-I, Type-II and Type-III seesaw respectively³. Finally the RG evolution

³ [41, 42] actually considered Type-I + Type-II case where they have one heavy right-handed fermion and a triplet Higgs added to the SM (and the MSSM also). However, we will consider the three types of seesaw scenarios separately.

equations for the charged lepton Yukawa matrix Y_e and the heavy particle Yukawa matrix Y_X and (here $X = N$ for Type-I, $X = \Delta$ for Type-II and $X = \Sigma$ for Type-III) can be given as

$$16\pi^2\beta_{Y_e} = Y_e F + \alpha_e Y_e, \quad (108)$$

$$16\pi^2\beta_{Y_X} = \begin{cases} Y_X G + \alpha_X Y_X & \text{Type-I \& III,} \\ Y_X G + G^T Y_X + \alpha_X Y_X & \text{Type-II,} \end{cases} \quad (109)$$

where F and G are defined as

$$F = D_e Y_e^\dagger Y_e + D_X Y_X^\dagger Y_X, \quad (110)$$

$$G = B_e Y_e^\dagger Y_e + B_X Y_X^\dagger Y_X. \quad (111)$$

The quantities D_e, D_X, B_e, B_X and α_e, α_X with the SM as the low energy effective theory are given in Table 4. The β -function for the heavy particle mass M_X is given as

$$16\pi^2\beta_{M_X} = \begin{cases} M_X \left(Y_X Y_X^\dagger \right)^T + \left(Y_X Y_X^\dagger \right) M_X + \alpha_{M_X} M_X & \text{Type-I \& III,} \\ \alpha'_{M_X} M_X^{-1} + \alpha_{M_X} M_X & \text{Type-II,} \end{cases} \quad (112)$$

with α_{M_X} and α'_{M_X} defined by

$$\alpha_{M_X} = \begin{cases} 0 & \text{Type-I,} \\ 4\Lambda_1 + \Lambda_2 + \text{Tr}[Y_\Delta^\dagger Y_\Delta] - \frac{9}{5}g_1^2 - 6g_2^2 & \text{Type-II,} \\ -12g_2^2 & \text{Type-III,} \end{cases} \quad (113)$$

$$\alpha'_{M_X} = 2\Lambda_4 m^2 + \frac{1}{2}|\Lambda_6|^2 \quad (\text{Type-II}), \quad (114)$$

where m is the bare mass of the SM Higgs ϕ and Λ_i s are the couplings associated with the triplet Higgs Δ , as given in Eq. (26).

After electroweak symmetry breaking, these coupled heavy fields will contribute to the generation of the light neutrino mass via seesaw, as given in Sec 2.2.1-2.2.3 for the three different seesaw scenarios

$$m_\nu = \begin{cases} -\frac{v^2}{2} Y_N^T M_N^{-1} Y_N & \text{Type-I,} \\ +\frac{v^2}{2} \frac{Y_\Delta \Lambda_6}{M_\Delta^2} & \text{Type-II,} \\ -\frac{v^2}{2} Y_\Sigma^T M_\Sigma^{-1} Y_\Sigma & \text{Type-III.} \end{cases} \quad (115)$$

In this section we would like to study the radiative corrections to the quantity

$$Q \equiv \begin{cases} Y_N^T M_N^{-1} Y_N & \text{Type-I,} \\ -\frac{Y_\Delta \Lambda_6}{M_\Delta^2} & \text{Type-II,} \\ Y_\Sigma^T M_\Sigma^{-1} Y_\Sigma & \text{Type-III,} \end{cases} \quad (116)$$

which is a well-defined quantity at different energy scales to denote the contribution to the light neutrino mass matrix from the coupled heavy fields and finally gives the light neutrino mass matrix as $m_\nu = -\frac{v^2}{2}Q$ after spontaneous symmetry breaking.

In the complete theory when the heavy fields are coupled, the RG evolution of Q can be obtained from the running of Y_X and M_X (running of Λ_6 is also required in case of Type-II seesaw, which can be obtained in [41, 43]) and finally the evolution of Q can be written as

$$16\pi^2\beta_Q = QP_Q + P_Q^T Q + \alpha_Q P_Q, \quad (117)$$

with P_Q defined as

$$P_Q = C'_e Y_e^\dagger Y_e + C'_X Y_X^\dagger Y_X. \quad (118)$$

The quantities C'_e, C'_X and α_Q for three seesaw scenarios with the SM as the low energy effective theory are also given in Table 4. Finally m_ν can be obtained from Q as $m_\nu = -\frac{v^2}{2}Q$, after spontaneous symmetry breaking.

In case of Type-I seesaw, the heavy fermion singlets do not have any gauge interactions and hence the presence of these singlets does not affect the running of the gauge couplings. However, for the other two seesaw scenarios, the RG evolution of the gauge couplings g_1, g_2, g_3 will depend on the number of heavy fields present. Let n be the number of heavy fields present at some energy scale. Then the evolution of the gauge couplings can be written as

$$16\pi^2\beta_{g_i} = b_i g_i^3, \quad (119)$$

where the values for b_i s in the three seesaw scenarios are tabulated in Table 5. As given in the Table 5, none of the heavy fields has any strong interactions and hence b_3 is always the same as its SM value. The Higgs triplets present in Type-II seesaw have $Y = 1$ and thus couple to both $U(1)_Y$ and $SU(2)_L$ gauge fields, while the triplet fermions in Type-III seesaw have $Y = 0$ and thus couple only to the $SU(2)_L$ gauge fields.

We do not give the evolution equations for the different Higgs couplings or for the up- and down-type quark Yukawa couplings here. The evolution equations for these couplings can be obtained in [61, 41, 107] for the different seesaw scenarios.

4.1 Sequential decoupling of heavy fields

The most general case of the high energy theories would have been the one when there are any arbitrary number of right-handed singlets in Type-I seesaw, or any number of triplet scalars in case of Type-II seesaw or arbitrary

	D_e	D_X	α_e
Type-I	3/2	-3/2	$T_I - \frac{9}{4}g_1^2 - \frac{9}{4}g_2^2$
Type-II	3/2	3/2	$T_{II} - \frac{9}{4}g_1^2 - \frac{9}{4}g_2^2$
Type-III	3/2	15/2	$T_{III} - \frac{9}{4}g_1^2 - \frac{9}{4}g_2^2$
	B_e	B_X	α_x
Type-I	-3/2	3/2	$T_I - \frac{9}{20}g_1^2 - \frac{9}{4}g_2^2$
Type-II	1/2	3/2	$T'_{II} - \frac{9}{10}g_1^2 - \frac{9}{2}g_2^2$
Type-III	5/2	5/2	$T_{III} - \frac{9}{20}g_1^2 - \frac{33}{4}g_2^2$
	C'_e	C'_X	α_Q
Type-I	-3/2	1/2	$2T_I - \frac{9}{10}g_1^2 - \frac{9}{2}g_2^2$
Type-II	1/2	3/2	$T_{II} - 2T'_{II} - 3g_2^2 + \lambda + f(\Lambda_i)$
Type-III	5/2	3/2	$2T_{III} - \frac{9}{10}g_1^2 - \frac{9}{2}g_2^2$
	C_e	C_X	α_κ
Type-I	-3/2	1/2	$2T_I + \lambda - 3g_2^2$
Type-II	-3/2	3/2	$2T_{II} + \lambda - 3g_2^2$
Type-III	-3/2	3/2	$2T_{III} + \lambda - 3g_2^2$

Table 4: The quantities defining the running of Y_e , Y_X , Q and κ for three types of seesaw scenarios [61, 41, 107]. Here $T_I \equiv \text{Tr}[Y_e^\dagger Y_e + Y_N^\dagger Y_N + 3Y_u^\dagger Y_u + 3Y_d^\dagger Y_d]$, $T_{II} \equiv \text{Tr}[Y_e^\dagger Y_e + 3Y_u^\dagger Y_u + 3Y_d^\dagger Y_d]$, $T'_{II} \equiv \text{Tr}[Y_\Delta^\dagger Y_\Delta]$ and $T_{III} \equiv \text{Tr}[Y_e^\dagger Y_e + 3Y_\Sigma^\dagger Y_\Sigma + 3Y_u^\dagger Y_u + 3Y_d^\dagger Y_d]$. The function $f(\Lambda_i)$ is defined as $f(\Lambda_i) = -8\Lambda_1 - 2\Lambda_2 - 4\Lambda_4 + 8\Lambda_5 - (4\Lambda_4 m^2 + |\Lambda_6|^2) M_\Delta^{-2}$, where m is the bare mass of the SM Higgs doublet ϕ and Λ_i are the couplings associated with the triplet Higgs Δ , as defined in Eq. (26).

	b_1	b_2	b_3
SM	41/10	-19/6	-7
Type-I	41/10	-19/6	-7
Type-II	$41/10 + 3n/5$	$-19/6 + 2n/3$	-7
Type-III	41/10	$-19/6 + 4n/3$	-7

Table 5: b_i in three types of seesaw scenarios with the SM as the low energy theory[61, 43, 107]. Here n is the number of heavy particles coupled to the theory at any particular energy scale.

number of fermion triplets in Type-III seesaw and these heavy fields decouple one by one at different thresholds.

Let us first consider the most general case of Type-I and Type-III seesaw when there are r heavy fields (singlets in case of Type-I and triplets in case of Type-III) having masses $M_1 < M_2 < \dots < M_{r-1} < M_r$. We consider

a quantity \mathbb{R} which contains the contribution from the coupled as well as decoupled heavy fields at any energy scale and is also well-defined at all μ , and then finally gives the light neutrino mass matrix as

$$\mathbb{m}_\nu = -\frac{v^2}{2}\mathbb{R} , \quad (120)$$

after electroweak symmetry breaking.

Above the heaviest mass M_r , all the r -fields are coupled to the theory and contribute to \mathbb{R} as

$$\mathbb{R}^{(r+1)} = Q^{(r+1)} , \quad (121)$$

where $Q^{(r+1)}$ denotes the contribution from the r coupled heavy fields and is given by

$$Q^{(r+1)} = Y_X^{T(r+1)} \mathbb{M}_X^{-1(r+1)} Y_X^{(r+1)} \quad (\mu > M_r) , \quad (122)$$

where $X \equiv \text{N}$ for Type-I and $X \equiv \Sigma$ for Type-III seesaw. Here $Y_X^{(r+1)}$ is a $[r \times n_F]$ dimensional matrix (n_F is the number of flavors, which is 3 in our case) given as

$$Y_X^{(r+1)} = \begin{pmatrix} (y_X)_{1,1} & \cdots & (y_X)_{1,n_F} \\ \vdots & & \vdots \\ (y_X)_{r,1} & \cdots & (y_X)_{r,n_F} \end{pmatrix} . \quad (123)$$

$\mathbb{M}_X^{(r+1)}$ is a $[r \times r]$ matrix and $Q^{(r+1)}$ as well as \mathbb{R} is a $[n_F \times n_F]$ dimensional matrix. We use the super-indices just to keep track of the number of coupled fields. Below the scale M_r , the heaviest of the heavy fields decouples from the theory. Integrating out this degree of freedom gives rise to an effective operator $\kappa^{(r)}$. The matching condition at $\mu = M_r$ is

$$\kappa_{ij}^{(r)} \Big|_{M_r} = 2(Y_X^T)^{(r+1)}_{ir} (M_r)^{-1} (Y_X)^{(r+1)}_{rj} \Big|_{M_r} , \quad (124)$$

where no summation over ' r ' is implied and $i, j \in \{1, 2, \dots, n_F\}$. This condition ensures the continuity of \mathbb{R} at $\mu = M_r$. In order to get the value of the threshold M_r , we need to write the above matching condition in the basis where $\mathbb{M}_X = \text{Diag}(M_1, M_2, \dots, M_r)$. Here it is worth mentioning that the matching scale has to be found carefully since \mathbb{M}_X itself runs with the energy scale, *i.e.* $M_i = M_i(\mu)$. The threshold scale M_i is therefore to be understood as $M_i(\mu = M_i)$.

In the energy range $M_{r-1} < \mu < M_r$, \mathbb{R} will be given as

$$\mathbb{R}^{(r)} = \frac{1}{2}\kappa^{(r)} + Q^{(r)}. \quad (125)$$

The first term in Eq. (125) is the contribution of the integrated out heavy fermion of mass M_r through the effective operator $\kappa^{(r)}$. The second term represents the contribution of the remaining $(r-1)$ heavy fermions, which are still coupled to the theory. $\mathbb{M}_X^{(r)}$ is now a $[(r-1) \times (r-1)]$ matrix while $\bar{Y}_X^{(r)}$ is a $[(r-1) \times n_F]$ dimensional matrix given as

$$Y_X \rightarrow \left\{ \begin{array}{c} \begin{pmatrix} (y_X)_{1,1} & \cdots & (y_X)_{1,n_F} \\ \vdots & & \vdots \\ (y_X)_{r-1,1} & \cdots & (y_X)_{r-1,n_F} \\ \hline 0 & \cdots & 0 \end{pmatrix} \\ M_r \text{ integrated out.} \end{array} \right\} = \bar{Y}_X^{(r)}, \quad (126)$$

Finally $\mathbb{M}_X^{(r)}$ and $\bar{Y}_X^{(r)}$ constitute $Q^{(r)}$, which is $[n_F \times n_F]$ dimensional. The matching condition at $\mu = M_{r-1}$ is

$$\kappa_{ij}^{(r-1)} \Big|_{M_{r-1}} = \kappa_{ij}^{(r)} \Big|_{M_{r-1}} + 2(Y_X^T)_{i(r-1)} (M_{r-1})^{-1} (\bar{Y}_X)_{(r-1)j} \Big|_{M_{r-1}}, \quad (127)$$

where no summation over ‘ $(r-1)$ ’ is to be taken.

Generalizing the above sequence, we can say that if we consider the intermediate energy region between the $(n-1)^{\text{th}}$ and the n^{th} threshold, i.e. $M_n > \mu > M_{n-1}$, then all the heavy fields from masses M_r down to M_n have been decoupled. In this region the Yukawa matrix $\bar{Y}_X^{(n)}$ will be $[(n-1) \times n_F]$ dimensional that couples the $(n-1)$ coupled fields with n_F flavors and will be given as

$$Y_X \rightarrow \left\{ \begin{array}{c} \begin{pmatrix} (y_X)_{1,1} & \cdots & (y_X)_{1,n_F} \\ \vdots & & \vdots \\ (y_X)_{n-1,1} & \cdots & (y_X)_{n-1,n_F} \\ \hline 0 & \cdots & 0 \\ \vdots & & \vdots \\ 0 & \cdots & 0 \end{pmatrix} \\ \text{heavy fermions with} \\ \text{masses } M_n \text{---} M_r \\ \text{integrated out.} \end{array} \right\} = \bar{Y}_X^{(n)}, \quad (128)$$

$\mathbb{M}_X^{(n)}$ will be $[(n-1) \times (n-1)]$ dimensional matrix involving the mass terms of all the coupled heavy fields. In this energy range \mathbb{R} will be

$$\mathbb{R}^{(n)} = \frac{1}{2}\kappa^{(n)} + Q^{(n)}, \quad (129)$$

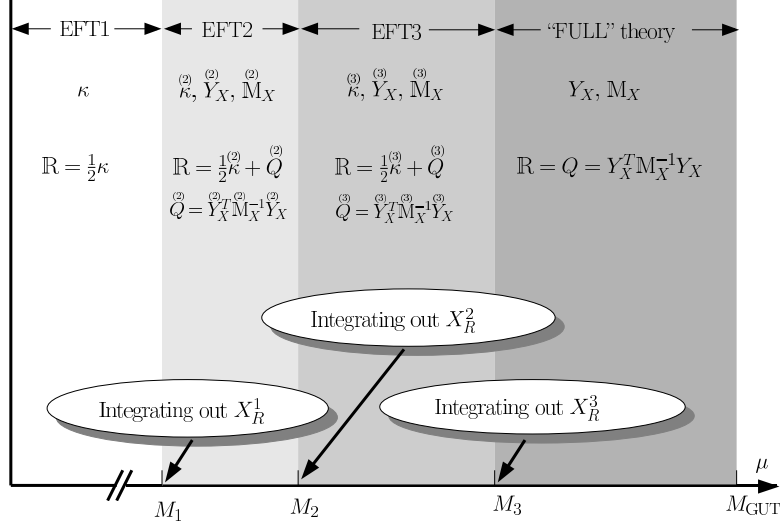


Figure 3: Sequential decoupling of the heavy fermions and construction of \mathbb{R} at different energy scales, for $r = 3$. Here $X \equiv N$ in case of Type-I and $X \equiv \Sigma$ for Type-III seesaw. Finally the light neutrino mass matrix is given as $m_\nu \equiv -\frac{v^2}{2}\mathbb{R}$ after spontaneous symmetry breaking, where v is the vacuum expectation value of the SM Higgs.

with

$$Q \equiv Y_X^{(n)T} M_X^{(n)-1} Y_X^{(n)}. \quad (130)$$

Note that \mathbb{R} , κ and Q are $[n_F \times n_F]$ matrices. The matching condition at $\mu = M_n$ is given by Eq. (127) with r replaced by $(n + 1)$.

At low energies $\mu < M_1$, when all the heavy fields are decoupled, $Q(\mu) = Q^{(1)}(\mu) = 0$ and $\mathbb{R}(\mu) = (1/2)\kappa^{(1)}(\mu)$. Fig. 3 shows the expressions for \mathbb{R} at different energy scales for the case of three heavy fermions *i.e.* for $r = 3$. Finally the light neutrino mass matrix m_ν is obtained as $m_\nu \equiv -\frac{v^2}{2}\mathbb{R}$, after the electroweak symmetry breaking.

In case of Type-I and Type-III seesaw, the concept of sequential decoupling is important since atleast two heavy fields are needed to generate the observed pattern of the light neutrino mass matrix and the heavy fermions can have non-degenerate masses in general. However, the case of Type-II seesaw is much simpler since only one heavy scalar triplet is sufficient to give rise to the small masses of the three active neutrinos and their mixings. Hence in this case one has only one threshold at $\mu = M_\Delta$ and \mathbb{R} at the two

different energy regimes will be given by

$$\mathbb{R} = \begin{cases} Q & (\mu > \mathbb{M}_\Delta) , \\ \frac{1}{2}\kappa & (\mu < \mathbb{M}_\Delta) , \end{cases} \quad (131)$$

where Q and κ are defined in Eq. (116) and Table 2 respectively. The matching conditions at $\mu = \mathbb{M}_\Delta$ will be given by

$$\kappa_{ij} \big|_{\mathbb{M}_\Delta} = -\frac{2}{\mathbb{M}_\Delta^2} \Lambda_6(Y_\Delta)_{ij} \big|_{\mathbb{M}_\Delta} , \quad (132)$$

$$\lambda \big|_{\mathbb{M}_\Delta} = \lambda \big|_{\mathbb{M}_\Delta} + \frac{2}{\mathbb{M}_\Delta^2} |\Lambda_6|^2 \big|_{\mathbb{M}_\Delta} . \quad (133)$$

Finally the light neutrino mass matrix \mathbb{m}_ν is obtained as $\mathbb{m}_\nu \equiv -\frac{v^2}{2}\mathbb{R}$, after the electroweak symmetry breaking.

For the sake of convenience and to be consistent with the existing literature, we will refer to $\mathbb{m}_\nu = -\frac{v^2}{2}\mathbb{R}$ as the effective light neutrino mass matrix at any energy scale, in the rest of the thesis. However, it must be understood that the quantity ‘ v ’ is present only after electroweak symmetry breaking and hence, strictly speaking, this relation is valid only in that energy regime, while \mathbb{R} is a well-defined quantity at all energy scales.

Finally, the RG evolution of the light neutrino mass matrix will be given by

$$16\pi^2\beta_{\mathbb{m}_\nu} = P^T \mathbb{m}_\nu + \mathbb{m}_\nu P + \alpha_\nu \mathbb{m}_\nu , \quad (134)$$

which is of the same form as Eq. (63). Here $P \equiv P_Q$, $\alpha_\nu \equiv \alpha_Q$ for $\mu > M_3$ and $P \equiv P_\kappa$, $\alpha_\nu \equiv \alpha_\kappa$ for $\mu < M_1$. In case of Type-I and Type-III seesaw, the running of the light neutrino masses in between the thresholds will be given by the running of both Q and κ , as shown in Eq. (129). For the energy scale $M_n > \mu > M_{n-1}$, the relevant quantities will be $Q^{(n)}$ and $\kappa^{(n)}$. The RG evolution of $Q^{(n)}$ can be obtained from Table 4 with the substitution $Y_X \rightarrow Y_X^{(n)}$ and $\mathbb{M}_X \rightarrow \mathbb{M}_X^{(n)}$. In case of Type-II seesaw there is only one threshold and the running of all relevant quantities contributing to the running of the neutrino mass matrix can be read off from Table 4.

It can be seen from the interaction of the heavy fields that they do not contribute to the 1-loop correction of the effective operator $\kappa^{(n)}$, even when they are coupled to the theory. So the evolution of the effective vertex $\kappa^{(n)}$ can be written as

$$16\pi^2\beta_{\kappa^{(n)}} = P_\kappa^T \kappa^{(n)} + \kappa^{(n)} P_\kappa + \alpha_\kappa \kappa^{(n)} \quad (135)$$

where

$$P_\kappa = C_e Y_e^\dagger Y_e + C_X Y_X^{(n)\dagger} Y_X^{(n)}, \quad (136)$$

and the quantities C_e , C_X and α_κ can be obtained from Table 4 and are independent of n , the number of heavy fields coupled at any energy scale.

4.2 RG evolution of neutrino mixing parameters

In order to evaluate the RG evolution of the light neutrino masses and the mixing parameters from the matrix evolutions, we proceed in the same way as done in Sec 3.1. Without the loss of generality, we choose to work in the basis in which $\mathbb{M}_X^{(n)}$ and $Y_e^\dagger Y_e$ are diagonal at the high energy.

As stated in the last section, for $\mu > M_3$ and $\mu < M_1$, the evolutions of m_ν will be given by the evolution of Q ($P = P_Q$) and κ ($P = P_\kappa$) respectively and hence the evolution of the angles, phases and light neutrino masses can be given in simple analytic forms. P and F , in Eqs.(134) and (108), are 3×3 matrices with the rows and columns representing generations. We denote the elements of P and F by P_{fg} and F_{fg} . If we write the evolution equations in the basis \mathcal{P}_δ , the apparent singularity at $\theta_{13} \rightarrow 0$ will be present, as can be seen from [42, 57]. As already discussed in Sec 3.1.3, this singularity can be removed using the basis \mathcal{P}_J [107]. Hence we discuss the RG evolution of the mixing angles, phases and the light neutrino masses in the \mathcal{P}_J basis in the following sections.

4.2.1 Evolution of mixing angles

Running of the two large mixing angles θ_{12} and θ_{23} in the basis \mathcal{P}_J , as given in Table 6, is also the same as that in the \mathcal{P}_δ basis since the quantities \mathcal{S}_{ij} and \mathcal{Q}_{ij}^\pm , defined as

$$\mathcal{Q}_{13}^\pm = \frac{|m_3 \pm m_1 e^{2i\phi_1}|^2}{\Delta m_{\text{atm}}^2 (1 + \zeta)}, \quad \mathcal{Q}_{23}^\pm = \frac{|m_3 \pm m_2 e^{2i\phi_2}|^2}{\Delta m_{\text{atm}}^2}, \quad \mathcal{Q}_{12}^\pm = \frac{|m_2 e^{2i\phi_2} \pm m_1 e^{2i\phi_1}|^2}{\Delta m_\odot^2}, \quad (137)$$

$$\mathcal{S}_{13} = \frac{m_1 m_3 \sin 2\phi_1}{\Delta m_{\text{atm}}^2 (1 + \zeta)}, \quad \mathcal{S}_{23} = \frac{m_2 m_3 \sin 2\phi_2}{\Delta m_{\text{atm}}^2}, \quad \mathcal{S}_{12} = \frac{m_1 m_2 \sin (2\phi_1 - 2\phi_2)}{\Delta m_\odot^2}, \quad (138)$$

depend on the mass eigenvalues and Majorana phases only, and not on the Dirac CP phase δ . However the running of θ_{13}^2 , as seen from the Table 6, depends on the quantities $\tilde{\mathcal{A}}_{ij}^\pm, \tilde{\mathcal{B}}_{ij}^\pm$ defined as

$$\tilde{\mathcal{A}}_{13}^\pm = \frac{4(m_1^2 + m_3^2) J'_{\text{CP}} \pm 8m_1 m_3 (J'_{\text{CP}} \cos 2\phi_1 + J_{\text{CP}} \sin 2\phi_1)}{a \Delta m_{\text{atm}}^2 (1 + \zeta)}, \quad (139)$$

$$\tilde{\mathcal{A}}_{23}^\pm = \frac{4(m_2^2 + m_3^2) J'_{\text{CP}} \pm 8m_2 m_3 (J'_{\text{CP}} \cos 2\phi_2 + J_{\text{CP}} \sin 2\phi_2)}{a \Delta m_{\text{atm}}^2}, \quad (140)$$

	$32\pi^2 \dot{\theta}_{12}$	$32\pi^2 \dot{\theta}_{23}$
P_{11}	$\mathcal{Q}_{12}^+ \sin 2\theta_{12}$	0
P_{22}	$-\mathcal{Q}_{12}^+ \sin 2\theta_{12} c_{23}^2$	$(\mathcal{Q}_{23}^+ c_{12}^2 + \mathcal{Q}_{13}^+ s_{12}^2) \sin 2\theta_{23}$
P_{33}	$-\mathcal{Q}_{12}^+ \sin 2\theta_{12} s_{23}^2$	$-(\mathcal{Q}_{23}^+ c_{12}^2 + \mathcal{Q}_{13}^+ s_{12}^2) \sin 2\theta_{23}$
$\text{Re } P_{21}$	$2\mathcal{Q}_{12}^+ \cos 2\theta_{12} c_{23}$	$(\mathcal{Q}_{23}^+ - \mathcal{Q}_{13}^+) \sin 2\theta_{12} s_{23}$
$\text{Re } P_{31}$	$-2\mathcal{Q}_{12}^+ \cos 2\theta_{12} s_{23}$	$(\mathcal{Q}_{23}^+ - \mathcal{Q}_{13}^+) \sin 2\theta_{12} c_{23}$
$\text{Re } P_{32}$	$\mathcal{Q}_{12}^+ \sin 2\theta_{12} \sin 2\theta_{23}$	$2(\mathcal{Q}_{23}^+ c_{12}^2 + \mathcal{Q}_{13}^+ s_{12}^2) \cos 2\theta_{23}$
$\text{Im } P_{21}$	$4\mathcal{S}_{12} c_{23}$	$2(\mathcal{S}_{23} - \mathcal{S}_{13}) \sin 2\theta_{12} s_{23}$
$\text{Im } P_{31}$	$-4\mathcal{S}_{12} s_{23}$	$2(\mathcal{S}_{23} - \mathcal{S}_{13}) \sin 2\theta_{12} c_{23}$
$\text{Im } P_{32}$	0	$4(\mathcal{S}_{23} c_{12}^2 + \mathcal{S}_{13} s_{12}^2)$

	$64\pi^2 \overrightarrow{\theta_{13}^2}$
P_{11}	0
P_{22}	$(\tilde{\mathcal{A}}_{23}^+ - \tilde{\mathcal{A}}_{13}^+) \sin 2\theta_{12} \sin 2\theta_{23}$
P_{33}	$-(\tilde{\mathcal{A}}_{23}^+ - \tilde{\mathcal{A}}_{13}^+) \sin 2\theta_{12} \sin 2\theta_{23}$
$\text{Re } P_{21}$	$4(\tilde{\mathcal{A}}_{13}^+ c_{12}^2 + \tilde{\mathcal{A}}_{23}^+ s_{12}^2) s_{23}$
$\text{Re } P_{31}$	$4(\tilde{\mathcal{A}}_{13}^+ c_{12}^2 + \tilde{\mathcal{A}}_{23}^+ s_{12}^2) c_{23}$
$\text{Re } P_{32}$	$2(\tilde{\mathcal{A}}_{23}^+ - \tilde{\mathcal{A}}_{13}^+) \sin 2\theta_{12} \cos 2\theta_{23}$
$\text{Im } P_{21}$	$4(\tilde{\mathcal{B}}_{13}^- c_{12}^2 + \tilde{\mathcal{B}}_{23}^- s_{12}^2) s_{23}$
$\text{Im } P_{31}$	$4(\tilde{\mathcal{B}}_{13}^- c_{12}^2 + \tilde{\mathcal{B}}_{23}^- s_{12}^2) c_{23}$
$\text{Im } P_{32}$	$2(\tilde{\mathcal{B}}_{23}^- - \tilde{\mathcal{B}}_{13}^-) \sin 2\theta_{12}$

Table 6: Coefficients of P_{fg} in the RG evolution equations of the mixing angles θ_{12} , θ_{13}^2 and θ_{23} , in the limit $\theta_{13} \rightarrow 0$ [57, 107].

$$\tilde{\mathcal{B}}_{13}^\pm = \frac{4(m_1^2 + m_3^2) J_{\text{CP}} \pm 8m_1 m_3 (J_{\text{CP}} \cos 2\phi_1 - J'_{\text{CP}} \sin 2\phi_1)}{a\Delta m_{\text{atm}}^2 (1 + \zeta)}, \quad (141)$$

$$\tilde{\mathcal{B}}_{23}^\pm = \frac{4(m_2^2 + m_3^2) J_{\text{CP}} \pm 8m_2 m_3 (J_{\text{CP}} \cos 2\phi_2 - J'_{\text{CP}} \sin 2\phi_2)}{a\Delta m_{\text{atm}}^2}, \quad (142)$$

where $a \equiv s_{12}c_{12}s_{23}c_{23}$. Clearly these quantities depend on J_{CP} , J'_{CP} in addition to the masses and Majorana phases and hence are basis-dependent. In the \mathcal{P}_J basis, all the quantities appearing in the evolution equations (139) – (142) have finite well-defined limits for $\theta_{13} \rightarrow 0$ and so will be θ_{13}^2 at any energy scale.

Table 7 shows the generic enhancement and suppression factors [57] for the evolution of the mixing angles, which is useful to estimate the RG evolution effects on the angles, when the active neutrinos are quasi-degenerate

	θ_{12}			θ_{23}		
	d.	n.h.	i.h.	d.	n.h.	i.h.
P_{11}	$\frac{m^2}{\Delta m_\odot^2}$	1	ζ^{-1}	$\mathcal{O}(\theta_{13})$	$\mathcal{O}(\theta_{13})$	$\mathcal{O}(\theta_{13})$
P_{22}	$\frac{m^2}{\Delta m_\odot^2}$	1	ζ^{-1}	$\frac{m^2}{\Delta m_{\text{atm}}^2}$	1	1
P_{33}	$\frac{m^2}{\Delta m_\odot^2}$	1	ζ^{-1}	$\frac{m^2}{\Delta m_{\text{atm}}^2}$	1	1
$\text{Re } P_{21}$	$\frac{m^2}{\Delta m_\odot^2}$	1	ζ^{-1}	$\frac{m^2}{\Delta m_{\text{atm}}^2}$	$\sqrt{\zeta}$	$\mathcal{O}(\theta_{13})$
$\text{Re } P_{31}$	$\frac{m^2}{\Delta m_\odot^2}$	1	ζ^{-1}	$\frac{m^2}{\Delta m_{\text{atm}}^2}$	$\sqrt{\zeta}$	$\mathcal{O}(\theta_{13})$
$\text{Re } P_{32}$	$\frac{m^2}{\Delta m_\odot^2}$	1	ζ^{-1}	$\frac{m^2}{\Delta m_{\text{atm}}^2}$	1	1
$\text{Im } P_{21}$	$\frac{m^2}{\Delta m_\odot^2}$	$\mathcal{O}(\theta_{13})$	ζ^{-1}	$\frac{m^2}{\Delta m_{\text{atm}}^2}$	$\sqrt{\zeta}$	$\mathcal{O}(\theta_{13})$
$\text{Im } P_{31}$	$\frac{m^2}{\Delta m_\odot^2}$	$\mathcal{O}(\theta_{13})$	ζ^{-1}	$\frac{m^2}{\Delta m_{\text{atm}}^2}$	$\sqrt{\zeta}$	$\mathcal{O}(\theta_{13})$
$\text{Im } P_{32}$	$\mathcal{O}(\theta_{13})$	$\mathcal{O}(\theta_{13})$	$\mathcal{O}(\theta_{13})$	$\frac{m^2}{\Delta m_{\text{atm}}^2}$	$\sqrt{\zeta}$	$\mathcal{O}(\theta_{13})$

	θ_{13}^2		
	d.	n.h.	i.h.
P_{11}	$\mathcal{O}(\theta_{13}^2)$	$\mathcal{O}(\theta_{13}^2)$	$\mathcal{O}(\theta_{13}^2)$
P_{22}	$\frac{m^2}{\Delta m_{\text{atm}}^2} \theta_{13}$	$\sqrt{\zeta} \theta_{13}$	$\mathcal{O}(\theta_{13}^2)$
P_{33}	$\frac{m^2}{\Delta m_{\text{atm}}^2} \theta_{13}$	$\sqrt{\zeta} \theta_{13}$	$\mathcal{O}(\theta_{13}^2)$
$\text{Re } P_{21}$	$\frac{m^2}{\Delta m_{\text{atm}}^2} \theta_{13}$	θ_{13}	θ_{13}
$\text{Re } P_{31}$	$\frac{m^2}{\Delta m_{\text{atm}}^2} \theta_{13}$	θ_{13}	θ_{13}
$\text{Re } P_{32}$	$\frac{m^2}{\Delta m_{\text{atm}}^2} \theta_{13}$	$\sqrt{\zeta} \theta_{13}$	$\mathcal{O}(\theta_{13}^2)$
$\text{Im } P_{21}$	$\frac{m^2}{\Delta m_{\text{atm}}^2} \theta_{13}$	θ_{13}	θ_{13}
$\text{Im } P_{31}$	$\frac{m^2}{\Delta m_{\text{atm}}^2} \theta_{13}$	θ_{13}	θ_{13}
$\text{Im } P_{32}$	$\frac{m^2}{\Delta m_{\text{atm}}^2} \theta_{13}$	$\sqrt{\zeta} \theta_{13}$	$\mathcal{O}(\theta_{13}^2)$

Table 7: Generic enhancement and suppression factors for the evolution of the angles, yielding an estimate of the size of the RG effect [57]. The table entries correspond to the terms in the mixing parameter RG evolution equations with the coefficient given by the first column. A ‘1’ indicates that there is no generic enhancement or suppression. ‘d.’ stands for a degenerate neutrino mass spectrum, *i.e.* $\Delta m_{\text{atm}}^2 \ll m_1^2 \sim m_2^2 \sim m_3^2 \sim m^2$. ‘n.h.’ denotes a normally hierarchical spectrum, *i.e.* $m_1 \ll m_2 \ll m_3$, and ‘i.h.’ means an inverted hierarchy, *i.e.* $m_3 \ll m_1 \lesssim m_2$.

($\Delta m_{\text{atm}}^2 \ll m_1^2 \sim m_2^2 \sim m_3^2 \sim m^2$ and this case is denoted by ‘d.’), or have normal mass hierarchy ($m_1 \ll m_2 \ll m_3$ and denoted by ‘n.h.’) or inverted mass hierarchy ($m_3 \ll m_1 \lesssim m_2$ and denoted by ‘i.h.’). From Table 7 we see that all terms in $\dot{\theta}_{12}$ are enlarged by $m^2/\Delta m_{\odot}^2$ for quasi-degenerate masses. Thus, there will be large RG effects, if the different terms do not cancel each other. The term involving $\text{Im } P_{32}$ is an exception, because its leading order is proportional to θ_{13} , so that it only plays a role in special cases. Also the terms involving $\text{Im } P_{21}$ and $\text{Im } P_{31}$ will have small contributions for small values of $(2\phi_1 - 2\phi_2)$. In the case of a strong normal hierarchy, there is no enhancement. For an inverted hierarchy, where the evolution is generically enhanced by ζ^{-1} , because the masses m_1 and m_2 are almost degenerate.

Both for θ_{23} and θ_{13}^2 , the evolution does not depend on P_{11} for $\theta_{13} = 0$. For these two mixing angles, the enhancement and suppression factors are similar (for θ_{13}^2 evolution, there is always an extra factor of θ_{13} compared to θ_{23} , as expected). The terms proportional to the other P_{fg} are enhanced by $m^2/\Delta m_{\text{atm}}^2$ in the degenerate case, so that effects are expected to be significant, but smaller than θ_{12} running. For both hierarchical spectra, the running is slow, as can be seen from Table 7. In case of diagonal P (or with P_{32} as the only non-zero off-diagonal entry) and inverted hierarchy, there will be no running for θ_{13}^2 if $\theta_{13} = 0$. However, this is no longer true if P_{21} or P_{31} is non-zero.

Thus in the evolution equations of the mixing angles, the generic characteristics of the terms which are proportional to the diagonal elements of P in the high energy theory is the same as those in the low energy effective theory, as already discussed in Eqs. (72)–(74) in Sec 3.1.1.

If the diagonal elements are equal, their contributions to the RG evolution equations cancel exactly. This follows from the fact that the mixing angles do not change under RG evolution, if P is the identity matrix and thus does not distinguish between the flavors. As can be seen in the next few sections, this statement holds also for the RG evolution of the CP phases. It provides a consistency check for the results. Interesting new effects occur for non-zero off-diagonal elements in P . Some of their coefficients in the evolution equations do not vanish for vanishing mixings, *e.g.* the coefficient of P_{21} in $\dot{\theta}_{12}$ in Table 6, and thus non-zero mixing angles are generated radiatively. This is in striking contrast to the region below the see-saw scale, as can be checked from Eqs. (72)–(74).

	$64\pi^2 \dot{J}_{\text{CP}}/a$	$64\pi^2 \dot{J}'_{\text{CP}}/a$
P_{11}	0	0
P_{22}	$-4a\mathcal{G}_s^-$	$2a(\mathcal{G}_0^- - 2\mathcal{G}_c^-)$
P_{33}	$4a\mathcal{G}_s^-$	$-2a(\mathcal{G}_0^- - 2\mathcal{G}_c^-)$
$\text{Re } P_{21}$	$4s_{23}\mathcal{G}_s^+$	$2s_{23}(\mathcal{G}_0^+ + 2\mathcal{G}_c^+)$
$\text{Re } P_{31}$	$4c_{23}\mathcal{G}_s^+$	$2c_{23}(\mathcal{G}_0^+ + 2\mathcal{G}_c^+)$
$\text{Re } P_{32}$	$-2 \sin 2\theta_{12} \cos 2\theta_{23} \mathcal{G}_s^-$	$\sin 2\theta_{12} \cos 2\theta_{23} (\mathcal{G}_0^- - 2\mathcal{G}_c^-)$
$\text{Im } P_{21}$	$2s_{23}(\mathcal{G}_0^+ - 2\mathcal{G}_c^+)$	$4s_{23}\mathcal{G}_s^+$
$\text{Im } P_{31}$	$2c_{23}(\mathcal{G}_0^+ - 2\mathcal{G}_c^+)$	$4c_{23}\mathcal{G}_s^+$
$\text{Im } P_{32}$	$\sin 2\theta_{12}(\mathcal{G}_0^- + 2\mathcal{G}_c^-)$	$-2 \sin 2\theta_{12}\mathcal{G}_s^-$

Table 8: Coefficients of P_{fg} in the RG evolution equations of the Jarlskog invariant J_{CP} , the quantity $J'_{\text{CP}} \equiv J_{\text{CP}} \cot \delta$, in the limit $\theta_{13} \rightarrow 0$. The convention used here is $a \equiv s_{12}c_{12}s_{23}c_{23}$, and $J_{\text{CP}} \equiv (a/2)s_{13}c_{13}^2 \sin \delta$ [107].

4.2.2 Evolution of $J_{\text{CP}}, J'_{\text{CP}}$

The coefficients for the RG evolution of J_{CP} and J'_{CP} are presented in Table 8, where the quantities $\mathcal{G}_{0,c,s}^\pm$ are given by

$$\mathcal{G}_0^\pm = \frac{m_2^2 + m_3^2}{\Delta m_{\text{atm}}^2} \pm \frac{m_1^2 + m_3^2}{\Delta m_{\text{atm}}^2(1 + \zeta)}, \quad (143)$$

$$\mathcal{G}_s^\pm = \frac{m_1 m_3 \sin 2\phi_1}{\Delta m_{\text{atm}}^2(1 + \zeta)} \pm \frac{m_2 m_3 \sin 2\phi_2}{\Delta m_{\text{atm}}^2}, \quad (144)$$

$$\mathcal{G}_c^\pm = \frac{m_1 m_3 \cos 2\phi_1}{\Delta m_{\text{atm}}^2(1 + \zeta)} \pm \frac{m_2 m_3 \cos 2\phi_2}{\Delta m_{\text{atm}}^2}. \quad (145)$$

Thus the quantities defined in Eqs. (143)–(145) are functions of masses and Majorana phases and hence are well-defined at all energies and at every point in the parameter space. Thus Table 8 shows that the running of $J_{\text{CP}}, J'_{\text{CP}}$ does not depend on themselves and hence independent of the Dirac CP phase δ upto $\mathcal{O}(\theta_{13}^0)$. It also shows that if P is identity (or proportional to identity), there will be no RG evolution, as expected.

From the generic enhancement and suppression factors for the RG evolution of J_{CP} and J'_{CP} given in Table 9 it can be seen that for degenerate light neutrino masses the coefficients are enlarged by the factor $m^2/\Delta m_{\text{atm}}^2$, for all P_{fg} except P_{11} . The leading contribution from P_{11} comes only at $\mathcal{O}(\theta_{13})$ and is also independent of the mass ordering of the neutrinos. For \dot{J}_{CP} , the contributions from the other two diagonal elements P_{22} and P_{33} are suppressed by $\sqrt{\zeta}$ for normal hierarchy, while for inverted hierarchy the leading contribution is only at $\mathcal{O}(\theta_{13})$. For \dot{J}'_{CP} the evolution is suppressed by ζ in both the cases.

	\dot{J}_{CP}/a			\dot{J}'_{CP}/a		
	d.	n.h.	i.h.	d.	n.h.	i.h.
P_{11}	$\mathcal{O}(\theta_{13})$	$\mathcal{O}(\theta_{13})$	$\mathcal{O}(\theta_{13})$	$\mathcal{O}(\theta_{13})$	$\mathcal{O}(\theta_{13})$	$\mathcal{O}(\theta_{13})$
P_{22}	$\frac{m^2}{\Delta m_{\text{atm}}^2}$	$\sqrt{\zeta}$	$\mathcal{O}(\theta_{13})$	$\frac{m^2}{\Delta m_{\text{atm}}^2}$	ζ	ζ
P_{33}	$\frac{m^2}{\Delta m_{\text{atm}}^2}$	$\sqrt{\zeta}$	$\mathcal{O}(\theta_{13})$	$\frac{m^2}{\Delta m_{\text{atm}}^2}$	ζ	ζ
$\text{Re } P_{21}$	$\frac{m^2}{\Delta m_{\text{atm}}^2}$	$\sqrt{\zeta}$	$\mathcal{O}(\theta_{13})$	$\frac{m^2}{\Delta m_{\text{atm}}^2}$	1	1
$\text{Re } P_{31}$	$\frac{m^2}{\Delta m_{\text{atm}}^2}$	$\sqrt{\zeta}$	$\mathcal{O}(\theta_{13})$	$\frac{m^2}{\Delta m_{\text{atm}}^2}$	1	1
$\text{Re } P_{32}$	$\frac{m^2}{\Delta m_{\text{atm}}^2}$	$\sqrt{\zeta}$	$\mathcal{O}(\theta_{13})$	$\frac{m^2}{\Delta m_{\text{atm}}^2}$	ζ	ζ
$\text{Im } P_{21}$	$\frac{m^2}{\Delta m_{\text{atm}}^2}$	1	1	$\frac{m^2}{\Delta m_{\text{atm}}^2}$	$\sqrt{\zeta}$	$\mathcal{O}(\theta_{13})$
$\text{Im } P_{31}$	$\frac{m^2}{\Delta m_{\text{atm}}^2}$	1	1	$\frac{m^2}{\Delta m_{\text{atm}}^2}$	$\sqrt{\zeta}$	$\mathcal{O}(\theta_{13})$
$\text{Im } P_{32}$	$\frac{m^2}{\Delta m_{\text{atm}}^2}$	ζ	ζ	$\frac{m^2}{\Delta m_{\text{atm}}^2}$	$\sqrt{\zeta}$	$\mathcal{O}(\theta_{13})$

Table 9: Generic enhancement and suppression factors for the evolution of J_{CP} and J'_{CP} , yielding an estimate of the size of the RG effect.

From Table 8 it can be seen that even if θ_{13} is zero to start with so that $J_{\text{CP}} = J'_{\text{CP}} = 0$ at the high scale, it can be generated radiatively. This is true even with a diagonal P , if P is not proportional to identity. This happens in the low energy effective theory also, as can be seen from Eqs. (102)–(103). However, if the diagonal elements are equal, their contributions cancel exactly and there will be no running at all. Table 8 also suggests that for non-zero off-diagonal elements of P , J_{CP} and J'_{CP} can be generated radiatively even when all the mixing angles are zero at the high scale and this is very different from what is expected in the effective theory below the seesaw scale.

4.2.3 Evolution of Majorana phases

The expressions for the running of the Majorana phases are the same in \mathcal{P}_J and \mathcal{P}_δ . Table 10 shows the running of the difference between the Majorana phases $|\phi_1 - \phi_2|$ [57, 107].

As can be seen from Table 11, the generic enhancement factors for the RG evolution of $(\phi_1 - \phi_2)$ are very similar to those for the running of θ_{12} , for degenerate light neutrino masses or for an inverted hierarchy. For normal hierarchy, there is no running if P is real, upto the zeroth order of θ_{13} , which implies that each of the Majorana phases runs by equal amount. The running of individual Majorana phases is discussed in [57]. The running of the Majorana phases is also important to understand the evolution of the mixing angles, since all the quantities defined in Eqs. (137)–(142) depend on the Majorana phases. RG evolution of the Majorana phases controls the

	$32\pi^2(\dot{\phi}_1 - \dot{\phi}_2)$
P_{11}	$-4\mathcal{S}_{12} \cos 2\theta_{12}$
P_{22}	$4\mathcal{S}_{12}c_{23}^2 \cos 2\theta_{12}$
P_{33}	$4\mathcal{S}_{12}s_{23}^2 \cos 2\theta_{12}$
$\text{Re } P_{21}$	$-8\mathcal{S}_{12}c_{23} \cos 2\theta_{12} \cot 2\theta_{12}$
$\text{Re } P_{31}$	$8\mathcal{S}_{12}s_{23} \cos 2\theta_{12} \cot 2\theta_{12}$
$\text{Re } P_{32}$	$-4\mathcal{S}_{12} \cos 2\theta_{12} \sin 2\theta_{23}$
$\text{Im } P_{21}$	$-4\mathcal{Q}_{12}^- c_{23} \cot 2\theta_{12}$
$\text{Im } P_{31}$	$4\mathcal{Q}_{12}^- s_{23} \cot 2\theta_{12}$
$\text{Im } P_{32}$	0

Table 10: Coefficients of P_{fg} in the RG evolution equations of the Majorana phase difference $(\phi_1 - \phi_2)$, in the limit $\theta_{13} \rightarrow 0$ [57, 107].

	$\dot{\phi}_1 - \dot{\phi}_2$		
	d.	n.h.	i.h.
P_{11}	$\frac{m^2}{\Delta m_{\odot}^2}$	$\mathcal{O}(\theta_{13})$	ζ^{-1}
P_{22}	$\frac{m^2}{\Delta m_{\odot}^2}$	$\mathcal{O}(\theta_{13})$	ζ^{-1}
P_{33}	$\frac{m^2}{\Delta m_{\odot}^2}$	$\mathcal{O}(\theta_{13})$	ζ^{-1}
$\text{Re } P_{21}$	$\frac{m^2}{\Delta m_{\odot}^2}$	$\mathcal{O}(\theta_{13})$	ζ^{-1}
$\text{Re } P_{31}$	$\frac{m^2}{\Delta m_{\odot}^2}$	$\mathcal{O}(\theta_{13})$	ζ^{-1}
$\text{Re } P_{32}$	$\frac{m^2}{\Delta m_{\odot}^2}$	$\mathcal{O}(\theta_{13})$	ζ^{-1}
$\text{Im } P_{21}$	$\frac{m^2}{\Delta m_{\odot}^2}$	1	ζ^{-1}
$\text{Im } P_{31}$	$\frac{m^2}{\Delta m_{\odot}^2}$	1	ζ^{-1}
$\text{Im } P_{32}$	$\mathcal{O}(\theta_{13})$	$\mathcal{O}(\theta_{13})$	$\mathcal{O}(\theta_{13})$

Table 11: Generic enhancement and suppression factors for the evolution of the difference of Majorana phases $(\phi_1 - \phi_2)$ [57].

running of J_{CP} , J'_{CP} also.

4.2.4 Evolution of light neutrino masses

Table 12 shows the RG evolution of the light neutrino masses. As can be seen, the coefficients are independent of J_{CP} , J'_{CP} and hence the expressions remain the same in the basis P_{δ} .

As is clear from Table 12, the evolution of m_i is proportional to itself. This is a general characteristic of the running of the mass eigenvalues at all energy scales. As a consequence, the mass eigenvalues can never run from a finite

	$16\pi^2 \dot{m}_1/m_1$	$16\pi^2 \dot{m}_2/m_2$	$16\pi^2 \dot{m}_3/m_3$
α_ν	1	1	1
P_{11}	$2c_{12}^2$	$2s_{12}^2$	0
P_{22}	$2s_{12}^2 c_{23}^2$	$2c_{12}^2 c_{23}^2$	$2s_{23}^2$
P_{33}	$2s_{12}^2 s_{23}^2$	$2c_{12}^2 s_{23}^2$	$2c_{23}^2$
$\text{Re } P_{21}$	$-2 \sin 2\theta_{12} c_{23}$	$2 \sin 2\theta_{12} c_{23}$	0
$\text{Re } P_{31}$	$2 \sin 2\theta_{12} s_{23}$	$-2 \sin 2\theta_{12} s_{23}$	0
$\text{Re } P_{32}$	$-2 \sin 2\theta_{23} s_{12}^2$	$-2 \sin 2\theta_{23} c_{12}^2$	$2 \sin 2\theta_{23}$
$\text{Im } P_{21}$	0	0	0
$\text{Im } P_{31}$	0	0	0
$\text{Im } P_{32}$	0	0	0

Table 12: Coefficients of P_{fg} in the RG evolution equations of the neutrino masses m_i $\{i = 1, 2, 3\}$, in the limit $\theta_{13} \rightarrow 0$ [57, 107].

value to zero or vice versa. However, this conclusion is very specific to the 1-loop running of the masses, and breaks down when the 2-loop contributions are taken into account [59].

As already discussed in Sec 3.1.2, below the see-saw scales, the evolution of the mass eigenvalues is, to a good approximation, described by a universal scaling caused by the flavor-independent part of the RG evolution equations proportional to α_ν . This flavor-independent term becomes smaller at high energies. Therefore, the flavor-dependent terms play a more important role above the see-saw scales. The importance of the flavor-dependent part increases if entries of Y_X become of order one. Thus between and above the see-saw scales, the running may become strongly influenced by the Yukawa couplings of the heavy fields.

RG evolution of Δm_\odot^2 and Δm_{atm}^2 , the quantities important for neutrino oscillations, can be obtained using Table 12, and is also discussed in [57].

4.2.5 Contribution from U_e

As already stated, we choose to work in the basis in which $\overset{(n)}{M}_X$ is diagonal. Hence from the Eqs. (20) and (51) we get that $\overset{(n)}{Y}_N$ and $\overset{(n)}{Y}_\Sigma$ will have non-zero off-diagonal components. So even if one starts with diagonal Y_e (*i.e.* $Y_e = \text{Diag}(y_e, y_\mu, y_\tau)$) at the high scale, non-zero off-diagonal elements of Y_e will be generated through Eqs. (108) and (110) since $\overset{(n)}{Y}_X^\dagger \overset{(n)}{Y}_X$ is not diagonal. Thus the contribution from U_e to U_{PMNS} , as given in Eq. (67), will be finite and there will be finite contribution to the running of masses and mixing above and between the thresholds through F and α_e . Since α_e is flavor

	$16\pi^2 \dot{\theta}_{12}^{U_e}$	$16\pi^2 \dot{\theta}_{13}^{U_e}$	$16\pi^2 \dot{\theta}_{23}^{U_e}$
F_{11}	0	0	0
F_{22}	0	0	0
F_{33}	0	0	0
$\text{Re } F_{21}$	$-c_{23}$	$-4s_{23}J'_{\text{CP}}/a$	0
$\text{Re } F_{31}$	s_{23}	$-4c_{23}J'_{\text{CP}}/a$	0
$\text{Re } F_{32}$	0	0	1
$\text{Im } F_{21}$	0	$-4s_{23}J_{\text{CP}}/a$	0
$\text{Im } F_{31}$	0	$-4c_{23}J_{\text{CP}}/a$	0
$\text{Im } F_{32}$	0	0	0

Table 13: Coefficients of F_{fg} in the RG evolution equations of all the angles $(\theta_{12}, \theta_{13}^2, \theta_{23})$, in the limit $\theta_{13} \rightarrow 0$. The convention used here is $a \equiv s_{12}c_{12}s_{23}c_{23}$, and $J_{\text{CP}} \equiv (a/2)s_{13}c_{13}^2 \sin \delta$. We neglect y_e and y_μ compared to y_τ , and take vanishing flavor phases [107].

diagonal, it will contribute to the running of y_e , y_μ and y_τ , while off-diagonal components of F will contribute additional terms in the β -functions of angles and phases. To evaluate the contributions from the off-diagonal components of Y_e , we consider the evolution of U_e as [57]

$$\frac{dU_e}{dt} = U_e X, \quad (146)$$

where $t \equiv \ln(\mu/\text{GeV})/16\pi^2$ and X is an anti-Hermitian matrix which can be determined from Eqs. (66) and (108) to have the form [57]

$$16\pi^2 X_{ij} = \frac{y_j^2 + y_i^2}{y_j^2 - y_i^2} (U_e^\dagger F U_e)_{ij} \quad (i \neq j), \quad (147)$$

where $y_1 = y_e$ and so on. The diagonal parts of X , which only influence the evolution of the unphysical phases, remain undetermined. Using Eqs. (68) and (146), one can write from Eq. (67)

$$\frac{dU_{\text{PMNS}}}{dt} = U_{\text{PMNS}} T + X^\dagger U_{\text{PMNS}}. \quad (148)$$

Using the expressions for T and X from Eqs. (69), (70) and (147), one gets the coupled equations for the angles and phases from Eq. (148). As suggested by Eq. (148), the contributions from the first term are already tabulated in Tables 6, 8, 10 and 12, and the contribution from the second term is the additional contribution because of the off-diagonal entries in $Y_e^\dagger Y_e$ generated

	$16\pi^2 J_{\text{CP}}^{U_e}$	$16\pi^2 J'_{\text{CP}}^{U_e}$	$16\pi^2 \phi_1^{U_e}$	$16\pi^2 \phi_2^{U_e}$
F_{11}	0	0	0	0
F_{22}	0	0	0	0
F_{33}	0	0	0	0
$\text{Re } F_{21}$	0	$-s_{23}a/2$	0	0
$\text{Re } F_{31}$	0	$-c_{23}a/2$	0	0
$\text{Re } F_{32}$	0	0	0	0
$\text{Im } F_{21}$	$-s_{23}a/2$	0	$c_{23}c_{12}/s_{12}$	$-c_{23}s_{12}/c_{12}$
$\text{Im } F_{31}$	$-c_{23}a/2$	0	$-s_{23}c_{12}/s_{12}$	$s_{23}s_{12}/c_{12}$
$\text{Im } F_{32}$	0	0	$-1/(c_{23}s_{23})$	$-1/(c_{23}s_{23})$

Table 14: Coefficients of F_{fg} in the RG evolution equations of J_{CP} , J'_{CP} and the Majorana phases ϕ_i in the limit $\theta_{13} \rightarrow 0$ [107].

in course of RG evolution. These additional terms in the β -functions of angles and phases are tabulated in Tables 13 and 14, respectively. These contributions will just get added to the P_{fg} contribution for the evolution of the quantities given in Tables 6, 8 and 10. Note that the F_{fg} coefficients are $\lesssim \mathcal{O}(1)$, whereas the P_{fg} coefficients are $\gtrsim \mathcal{O}(m_i^2/\Delta m_{\text{atm}}^2)$. Since the running is significant only when $m_i^2 \gg \Delta m_{\text{atm}}^2$, in almost all the region of interest P_{fg} contributions dominate over the F_{fg} contribution.⁴

In Type-II seesaw, we consider only one triplet Higgs, and so M_Δ is a number and hence from Eq. (32) we see that Y_Δ may be chosen to be diagonal in general. Thus if Y_e is chosen to be diagonal at high energy, it will remain so and the same procedure as in Sec 3.1 can be followed with the change that here the running of Q is to be considered instead of κ .

Note that the analytical expressions obtained in Eq. (137) onwards, and those given in the tables, are valid only in the two extreme regions $\mu > M_3$ and $\mu < M_1$. For the intermediate energy scales, m_ν will receive contributions from both $\kappa^{(n)}$ and $Q^{(n)}$. In the SM these two quantities have non-identical evolutions, as seen from Eqs. (135) and (117), and therefore the net evolution of Y_e and m_ν is rather complicated and needs numerical studies.

Quantitative studies have been made to show that the threshold effects may have dramatic consequences and can make many high energy neutrino mass models compatible with the current oscillation data at low energy which would have been excluded otherwise and vice versa. To illustrate the fact, bimaximal mixing scenario ($\theta_{12} = \theta_{23} = \pi/4$, $\theta_{13} = 0$) [108] is not allowed by

⁴ If the running of the mixing angles θ_{12} and θ_{23} is large to make the angles close to zero or $\pi/2$ at some energy scale, the coefficients of some of the $\text{Im } F_{fg}$ may become large for $\dot{\phi}_i$, as can be seen from Table 14.

the current oscillation experiment data, as can be seen from Table 1. But it is possible to make this symmetry allowed at the high energy when threshold effects are taken into account, in case of both Type-I [105] and Type-III [107] seesaw.

5 Conclusions

In the framework of the standard model (SM) of particle physics, neutrinos are massless at the tree level as well as at loop level. Hence one has to extend the SM in order to explain the tiny active neutrino masses observed experimentally. The most favored mechanisms to generate such small neutrino masses are the seesaw mechanisms, in which small active neutrino masses are generated at some high energy scale.

All these models predict the light neutrino masses and the mixing parameters at some high energy which corresponds, in some way, to the mass scale of the new fields added to the SM to generate the light neutrino masses. But since the experimental data are available at the laboratory energy scale, one needs to include the effects of renormalization group (RG) evolution. Unlike the quark sector where RG evolutions are quite small because of the hierarchical quark masses and small mixings, the effect of RG evolution on the neutrino masses and the mixing parameters are important. In this paper we reviewed the seesaw mechanisms that generate the light neutrino masses and the RG evolution of the neutrino masses and mixing parameters in the seesaw scenarios.

The low energy effective operator to generate the light neutrino masses is the same for all the three types of seesaws and thus the RG evolution of the parameters depend only on the effective theory *i.e.* whether it is the SM or the Minimal Supersymmetric Standard Model (MSSM), which has been discussed in detail. The Pontecorvo-Maki-Nakagawa-Sakata (PMNS) parametrization of the neutrino mixing matrix is characterized by the fact that at $\theta_{13} = 0$, the Dirac CP phase δ is unphysical. This leads to the singular behavior of δ at $\theta_{13} = 0$. However, this singularity is unphysical, since all the elements of the neutrino mixing matrix U_{PMNS} are continuous at $\theta_{13} = 0$, and in fact the value of δ there should be immaterial. The singularity also creeps in the running of θ_{13} , while evolution of the other parameters is well-behaved. However, as discussed here, it is possible to express the RG evolution of all the parameters as continuous first-order differential equations if one chooses the basis to be $\mathcal{P}_J = \{m_i, \theta_{12}, \theta_{23}, \theta_{13}^2, \phi_i, J_{\text{CP}}, J'_{\text{CP}}\}$, instead of the conventional $\mathcal{P}_\delta \equiv \{m_i, \theta_{ij}, \phi_i, \delta\}$ basis. The evolution equations in the new \mathcal{P}_J basis and their approximate integrated forms have also been discussed.

When the RG evolution in the high energy theory is considered, one needs to take the effects of the heavy fields into account carefully, since the evolution will depend on their interactions with the other fields. Moreover, the heavy fields will decouple from the theory step by step at their respective mass scales and start contributing through the effective operators, so the threshold effects are to be considered and matching conditions are to be imposed. We considered the evolution in three seesaw scenarios and with the SM as the effective theory. For energy regimes higher than the mass of the heaviest particle and lower than the lightest one, the evolution can be expressed by simple analytic formulae and qualitative understanding of the RG evolution is possible independent of the low energy theory considered. However, the final evolution of any parameter will depend on the choice of the high energy seesaw scenario, as well as the low energy effective theory.

RG evolution can have dramatic effects on the masses and the mixing parameters in the neutrino sector, especially when threshold effects are taken into account. These effects can make many high energy neutrino mass models compatible with the current oscillation data at low energy which would have been excluded otherwise and vice versa. Since precision data is expected from the upcoming neutrino experiments, it is important to consider the RG evolution effects while talking about the neutrino mass models, and it then be possible to exclude different classes of models and to gather knowledge about the possible high scale symmetries.

Acknowledgement

S.R. would like to thank Prof. Amol Dighe for his useful suggestions, guidance and comments on the final manuscript. The work was partially supported by the Max Planck – India Partnergroup project between Tata Institute of Fundamental Research and Max Planck Institute for Physics.

Appendix: Diagonalization of neutrino mass matrix

To check the diagonalization procedure, let us consider the case when there are arbitrary ‘ n ’ number of heavy right-handed neutrinos and three active neutrino species. Then the neutrino mass matrix \mathcal{M}_ν is a $n \times n$ matrix given by Eq. (10) as

$$\mathcal{M}_\nu = \begin{pmatrix} 0 & \mathbf{m}_D \\ \mathbf{m}_D^T & \mathbf{M}_N \end{pmatrix}, \quad (\text{A.1})$$

where \mathfrak{m}_D is a $3 \times n$ matrix, and \mathbb{M}_N is $n \times n$. Let us now consider the unitary transformation

$$\begin{pmatrix} A & B \\ C & D \end{pmatrix}^\dagger \begin{pmatrix} 0 & \mathfrak{m}_D \\ \mathfrak{m}_D^T & \mathbb{M}_N \end{pmatrix} \begin{pmatrix} A & B \\ C & D \end{pmatrix}^* = \begin{pmatrix} \mathfrak{m}_1 & 0 \\ 0 & \mathfrak{m}_2 \end{pmatrix} \quad (\text{A.2})$$

that diagonalize the mass matrix. From Eq. (A.2) one gets

$$\mathfrak{m}_1 = A^\dagger \mathfrak{m}_D C^* + C^\dagger \mathfrak{m}_D^T A^* + C^\dagger \mathbb{M}_N C^*, \quad (\text{A.3})$$

$$\mathfrak{m}_2 = B^\dagger \mathfrak{m}_D D^* + D^\dagger \mathfrak{m}_D^T B^* + D^\dagger \mathbb{M}_N D^*. \quad (\text{A.4})$$

The relation in Eq. (A.4) gives

$$D \mathfrak{m}_2 D^T = \Delta_D + (\mathbb{1} - \epsilon) \mathbb{M}_N (\mathbb{1} - \epsilon^T), \quad (\text{A.5})$$

where $\Delta_D \equiv DB^\dagger \mathfrak{m}_D (\mathbb{1} - \epsilon^T) + (\mathbb{1} - \epsilon) \mathfrak{m}_D^T B^* D^T$. Here we have used the fact that $\mathbb{M}_N \gg \mathfrak{m}_D$ and defined $DD^\dagger = \mathbb{1} - \epsilon$, where $\epsilon = (\mathfrak{m}_D \mathbb{M}_N^{-1})^n$, n to be determined. The unitarity condition gives $B^\dagger B + D^\dagger D = \mathbb{1}$, which implies $B = \mathcal{O}(\epsilon^{1/2})$. The same holds for C . In a similar way one has from unitarity $AA^\dagger = \mathbb{1} - \epsilon$. Eq. (A.2) also gives

$$A^\dagger \mathfrak{m}_D D^* + C^\dagger \mathfrak{m}_D^T B^* + C^\dagger \mathbb{M}_N D^* = 0, \quad (\text{A.6})$$

which reduces to

$$\begin{aligned} A^\dagger \mathfrak{m}_D + C^\dagger \mathbb{M}_N &= C^\dagger \mathfrak{m}_D^T B^* (D^*)^{-1} \\ &= \mathcal{O}(\epsilon^{1/2}) \mathfrak{m}_D^T \mathcal{O}(\epsilon^{1/2}) D^T (\mathbb{1} + \epsilon^T). \end{aligned} \quad (\text{A.7})$$

Thus

$$C^\dagger = \mathcal{O}(\epsilon) - A^\dagger \mathfrak{m}_D \mathbb{M}_N^{-1}, \quad (\text{A.8})$$

which in turn shows that $\epsilon \sim \mathcal{O}((\mathfrak{m}_D/\mathbb{M}_N)^2)$. Hence $B \sim C \sim \mathcal{O}(\mathfrak{m}_D/\mathbb{M}_N)$ and $D \mathfrak{m}_2 D^T = \mathbb{M}_N + \mathcal{O}(\mathfrak{m}_D^2/\mathbb{M}_N)$, which is the same as that given in Eq. (12) in Sec 2. From Eq. (A.3), keeping terms upto $\mathcal{O}(\mathfrak{m}_D/\mathbb{M}_N)$, one gets

$$A \mathfrak{m}_1 A^T = -\mathfrak{m}_D \mathbb{M}_N^{-1} \mathfrak{m}_D^T, \quad (\text{A.9})$$

and this is nothing but the seesaw relation, quoted in Eq. (11). Related discussions can also be found in [109].

References

- [1] Y. Fukuda *et al.* [Super-Kamiokande Collaboration], *Phys. Rev. Lett.* **81**, 1562 (1998).
- [2] Ahn, M. H. et al. *Phys. Rev.* **D74**, 072003 (2006).
- [3] Michael, D. G. et al. *Phys. Rev. Lett.* **97**, 191801 (2006).
- [4] Schwetz, T., Tortola, M., and Valle, J. W. F. *New J. Phys.* **10**, 113011 (2008).
- [5] Apollonio, M. et al. *Eur. Phys. J.* **C27**, 331–374 (2003).
- [6] F. Dydak *et al.*, *Phys. Lett. B* **134**, 281 (1984).
- [7] P. Astier *et al.* [NOMAD Collaboration], *Phys. Lett. B* **570**, 19 (2003) [arXiv:hep-ex/0306037].
- [8] Q. R. Ahmad *et al.* [SNO Collaboration], *Phys. Rev. Lett.* **87**, 071301 (2001) [arXiv:nucl-ex/0106015].
- [9] Fukuda, S. et al. *Phys. Rev. Lett.* **86**, 5656–5660 (2001).
- [10] Bahcall, J. N., Gonzalez-Garcia, M. C., and Pena-Garay, C. *JHEP* **07**, 054 (2002).
- [11] T. Araki *et al.* [KamLAND Collaboration], *Phys. Rev. Lett.* **94**, 081801 (2005).
- [12] B. Pontecorvo, *Sov. Phys. JETP* **7**, 172 (1958) [*Zh. Eksp. Teor. Fiz.* **34**, 247 (1957)].
- [13] B. Pontecorvo, *Sov. Phys. JETP* **26**, 984 (1968) [*Zh. Eksp. Teor. Fiz.* **53**, 1717 (1967)].
- [14] V. N. Gribov and B. Pontecorvo, *Phys. Lett. B* **28**, 493 (1969).
- [15] Z. Maki, M. Nakagawa and S. Sakata, *Prog. Theor. Phys.* **28**, 870 (1962).
- [16] G. L. Fogli, E. Lisi, A. Marrone, A. Palazzo and A. M. Rotunno, *Phys. Rev. Lett.* **101**, 141801 (2008) [arXiv:0806.2649 [hep-ph]].
- [17] A. Bandyopadhyay, S. Choubey, S. Goswami, S. T. Petcov and D. P. Roy, arXiv:0804.4857 [hep-ph].

- [18] M. Maltoni and T. Schwetz, arXiv:0812.3161 [hep-ph].
- [19] G. L. Fogli, E. Lisi, A. Marrone, A. Palazzo and A. M. Rotunno, Phys. Rev. Lett. **101**, 141801 (2008) [arXiv:0806.2649 [hep-ph]].
- [20] Kraus, C. et al. *Eur. Phys. J.* **C40**, 447–468 (2005).
- [21] R. G. H. Robertson [KATRIN Collaboration], J. Phys. Conf. Ser. **120**, 052028 (2008).
- [22] Klapdor-Kleingrothaus, H. V. et al. *Eur. Phys. J.* **A12**, 147–154 (2001).
- [23] Komatsu, E. et al. *Astrophys. J. Suppl.* **180**, 330–376 (2009).
- [24] S. Hannestad, Phys. Rev. Lett. **95**, 221301 (2005) [arXiv:astro-ph/0505551].
- [25] R. N. Mohapatra and J. W. F. Valle, Phys. Rev. D **34**, 1642 (1986).
- [26] A. Zee, Phys. Lett. B **93**, 389 (1980) [Erratum-ibid. B **95**, 461 (1980)];
- [27] R. N. Mohapatra and P. B. Pal, “*Massive neutrinos in Physics and Astrophysics*” (Third Edi.), World Scientific, 2004.
- [28] A. Zee, Phys. Lett. B **161**, 141 (1985); A. Zee, Nucl. Phys. B **264**, 99 (1986); K. S. Babu, Phys. Lett. B **203**, 132 (1988).
- [29] K. S. Babu, S. Nandi and Zurab Tavartkiladze, arXiv:0905.2710 [hep-ph].
- [30] S. Weinberg, Phys. Rev. Lett. **43**, 1566 (1979).
- [31] Minkowski, P. *Phys. Lett.* **B67**, 421 (1977).
- [32] Yanagida, T. *Proceedings of the Workshop on the Unified Theory and the Baryon Number in the Universe*. KEK, Tsukuba, Japan, (1979).
- [33] Gell-Mann, M, R. P. and Slansky, R. *Complex spinors and unified theories*. Supergravity. North Holland, Amsterdam, (1979).
- [34] Glashow, S. L. *The future of elementary particle physics*. Proceedings of the 1979 Cargèse Summer Institute on Quarks and Leptons. Plenum Press, New York, (1980).
- [35] Mohapatra, R. N. and Senjanovic, G. *Phys. Rev. Lett.* **44**, 912 (1980).

- [36] J. Kersten, *Diploma Thesis* (2001).
- [37] Magg, M. and Wetterich, C. *Phys. Lett.* **B94**, 61 (1980).
- [38] Lazarides, G., Shafi, Q., and Wetterich, C. *Nucl. Phys.* **B181**, 287 (1981).
- [39] Foot, R., Lew, H., He, X. G., and Joshi, G. C. *Z. Phys.* **C44**, 441 (1989).
- [40] Ma, E. and Roy, D. P. *Nucl. Phys.* **B644**, 290–302 (2002).
- [41] M. A. Schmidt, *Phys. Rev. D* **76**, 073010 (2007) [arXiv:0705.3841 [hep-ph]].
- [42] M. A. Schmidt, *Diploma Thesis* (2004).
- [43] W. Chao and H. Zhang, *Phys. Rev. D* **75**, 033003 (2007) [arXiv:hep-ph/0611323].
- [44] I. Gogoladze, N. Okada and Q. Shafi, *Phys. Rev. D* **78**, 085005 (2008) [arXiv:0802.3257 [hep-ph]].
- [45] Bajc, B. and Senjanovic, G. *JHEP* **08**, 014 (2007).
- [46] Bajc, B., Nemevsek, M., and Senjanovic, G. *Phys. Rev.* **D76**, 055011 (2007).
- [47] Abada, A., Biggio, C., Bonnet, F., Gavela, M. B., and Hambye, T. *JHEP* **12**, 061 (2007).
- [48] Franceschini, R., Hambye, T., and Strumia, A. *Phys. Rev.* **D78**, 033002 (2008).
- [49] del Aguila, F. and Aguilar-Saavedra, J. A. *Nucl. Phys.* **B813**, 22–90 (2009).
- [50] Abada, A., Biggio, C., Bonnet, F., Gavela, M. B., and Hambye, T. *Phys. Rev.* **D78**, 033007 (2008).
- [51] Ma, E. and Suematsu, D. *Mod. Phys. Lett.* **A24**, 583–589 (2009).
- [52] Fileviez Perez, P. *Phys. Rev.* **D76**, 071701 (2007).
- [53] Dorsner, I. and Fileviez Perez, P. *JHEP* **06**, 029 (2007).

- [54] Mohapatra, R. N., Okada, N., and Yu, H.-B. *Phys. Rev.* **D78**, 075011 (2008).
- [55] M. Malinsky, T. Ohlsson and H. Zhang, *Phys. Rev. D* **79**, 073009 (2009) [arXiv:0903.1961 [hep-ph]].
- [56] M. Malinsky, T. Ohlsson, Z. Z. Xing and H. Zhang, *Phys. Lett. B* **679**, 242 (2009) [arXiv:0905.2889 [hep-ph]].
- [57] S. Antusch, J. Kersten, M. Lindner, M. Ratz and M. A. Schmidt, *JHEP* **0503**, 024 (2005) [arXiv:hep-ph/0501272];
- [58] S. Antusch, M. Drees, J. Kersten, M. Lindner and M. Ratz, *Phys. Lett. B* **525**, 130 (2002) [arXiv:hep-ph/0110366].
- [59] S. Davidson, G. Isidori and A. Strumia, *Phys. Lett. B* **646**, 100 (2007) [arXiv:hep-ph/0611389].
- [60] M. E. Peskin and D. V. Schroeder, “*An Introduction to Quantum Field Theory*,” (Addison-Wesley, Reading, Massachusetts, 1997).
- [61] S. Antusch, J. Kersten, M. Lindner and M. Ratz, *Nucl. Phys. B* **674**, 401 (2003) [arXiv:hep-ph/0305273].
- [62] A. Dighe, S. Goswami and S. Ray, arXiv:0810.5680 [hep-ph].
- [63] A. Dighe, S. Goswami and P. Roy, *Phys. Rev. D* **73**, 071301 (2006) [arXiv:hep-ph/0602062].
- [64] A. Dighe, S. Goswami and W. Rodejohann, *Phys. Rev. D* **75**, 073023 (2007) [arXiv:hep-ph/0612328].
- [65] A. Dighe, S. Goswami and P. Roy, *Phys. Rev. D* **76**, 096005 (2007) [arXiv:0704.3735 [hep-ph]].
- [66] J. R. Ellis and S. Lola, *Phys. Lett. B* **458**, 310 (1999) [arXiv:hep-ph/9904279].
- [67] Chankowski, P. H., Krolikowski, W., and Pokorski, S. *Phys. Lett.* **B473**, 109–117 (2000).
- [68] P. H. Chankowski and Z. Pluciennik, *Phys. Lett. B* **316**, 312 (1993) [arXiv:hep-ph/9306333]; P. H. Chankowski and S. Pokorski, *Int. J. Mod. Phys. A* **17**, 575 (2002) [arXiv:hep-ph/0110249].

- [69] K. S. Babu, C. N. Leung and J. T. Pantaleone, Phys. Lett. B **319**, 191 (1993) [arXiv:hep-ph/9309223].
- [70] S. Antusch, M. Drees, J. Kersten, M. Lindner and M. Ratz, Phys. Lett. B **519**, 238 (2001) [arXiv:hep-ph/0108005].
- [71] T. Fukuyama and N. Okada, JHEP **0211**, 011 (2002) [arXiv:hep-ph/0205066].
- [72] M. Tanimoto, Phys. Lett. B **360**, 41 (1995) [arXiv:hep-ph/9508247].
- [73] N. Haba, N. Okamura and M. Sugiura, Prog. Theor. Phys. **103**, 367 (2000) [arXiv:hep-ph/9810471].
- [74] K. R. S. Balaji, A. S. Dighe, R. N. Mohapatra and M. K. Parida, Phys. Rev. Lett. **84**, 5034 (2000) [arXiv:hep-ph/0001310]; K. R. S. Balaji, A. S. Dighe, R. N. Mohapatra and M. K. Parida, Phys. Lett. B **481**, 33 (2000) [arXiv:hep-ph/0002177].
- [75] K. R. S. Balaji, R. N. Mohapatra, M. K. Parida and E. A. Paschos, Phys. Rev. D **63**, 113002 (2001) [arXiv:hep-ph/0011263].
- [76] R. N. Mohapatra, M. K. Parida and G. Rajasekaran, Phys. Rev. D **69**, 053007 (2004) [arXiv:hep-ph/0301234].
- [77] S. K. Agarwalla, M. K. Parida, R. N. Mohapatra and G. Rajasekaran, Phys. Rev. D **75**, 033007 (2007) [arXiv:hep-ph/0611225].
- [78] F. Vissani, arXiv:hep-ph/9708483.
- [79] G. C. Branco, M. N. Rebelo and J. I. Silva-Marcos, Phys. Rev. Lett. **82**, 683 (1999) [arXiv:hep-ph/9810328].
- [80] J. A. Casas, J. R. Espinosa, A. Ibarra and I. Navarro, Nucl. Phys. B **556**, 3 (1999) [arXiv:hep-ph/9904395].
- [81] J. A. Casas, J. R. Espinosa, A. Ibarra and I. Navarro, Nucl. Phys. B **569**, 82 (2000) [arXiv:hep-ph/9905381].
- [82] N. Haba, Y. Matsui, N. Okamura and M. Sugiura, Prog. Theor. Phys. **103**, 145 (2000) [arXiv:hep-ph/9908429].
- [83] R. Adhikari, E. Ma and G. Rajasekaran, Phys. Lett. B **486**, 134 (2000) [arXiv:hep-ph/0004197].

- [84] A. S. Joshipura, S. D. Rindani and N. N. Singh, Nucl. Phys. B **660**, 362 (2003) [arXiv:hep-ph/0211378].
- [85] A. S. Joshipura and S. Mohanty, Phys. Rev. D **67**, 091302 (2003) [arXiv:hep-ph/0302181].
- [86] Z. Z. Xing and H. Zhang, Commun. Theor. Phys. **48**, 525 (2007) [arXiv:hep-ph/0601106].
- [87] S. T. Petcov, T. Shindou and Y. Takanishi, Nucl. Phys. B **738**, 219 (2006) [arXiv:hep-ph/0508243].
- [88] A. S. Joshipura, Phys. Lett. B **543**, 276 (2002) [arXiv:hep-ph/0205038].
- [89] A. S. Joshipura and S. D. Rindani, Phys. Rev. D **67**, 073009 (2003) [arXiv:hep-ph/0211404].
- [90] J. W. Mei and Z. Z. Xing, Phys. Rev. D **70**, 053002 (2004) [arXiv:hep-ph/0404081].
- [91] S. Lola, Acta Phys. Polon. B **31**, 1253 (2000) [arXiv:hep-ph/0005093].
- [92] N. Haba and N. Okamura, Eur. Phys. J. C **14**, 347 (2000) [arXiv:hep-ph/9906481].
- [93] E. Ma, J. Phys. G **25**, L97 (1999) [arXiv:hep-ph/9907400].
- [94] N. Haba, Y. Matsui, N. Okamura and T. Suzuki, Phys. Lett. B **489**, 184 (2000) [arXiv:hep-ph/0005064].
- [95] P. H. Chankowski, W. Krolkowski and S. Pokorski, Phys. Lett. B **473**, 109 (2000) [arXiv:hep-ph/9910231].
- [96] J. T. Pantaleone, T. K. Kuo and G. H. Wu, Phys. Lett. B **520**, 279 (2001) [arXiv:hep-ph/0108137].
- [97] S. Luo and Z. Z. Xing, Phys. Lett. B **637**, 279 (2006) [arXiv:hep-ph/0603091].
- [98] F. Plentinger and W. Rodejohann, Phys. Lett. B **625**, 264 (2005) [arXiv:hep-ph/0507143].
- [99] A. Dighe, S. Goswami and P. Roy, Phys. Rev. D **76**, 096005 (2007) [arXiv:0704.3735 [hep-ph]].

- [100] M. Hirsch, E. Ma, J. C. Romao, J. W. F. Valle and A. Villanova del Moral, Phys. Rev. D **75**, 053006 (2007) [arXiv:hep-ph/0606082].
- [101] M. A. Schmidt and A. Y. Smirnov, Phys. Rev. D **74**, 113003 (2006) [arXiv:hep-ph/0607232].
- [102] S. Goswami, S. T. Petcov, S. Ray and W. Rodejohann, Phys. Rev. D **80**, 053013 (2009) [arXiv:0907.2869 [hep-ph]].
- [103] S. F. King and N. N. Singh, Nucl. Phys. B **591**, 3 (2000) [arXiv:hep-ph/0006229].
- [104] S. Antusch, J. Kersten, M. Lindner and M. Ratz, Phys. Lett. B **538**, 87 (2002) [arXiv:hep-ph/0203233].
- [105] S. Antusch, J. Kersten, M. Lindner and M. Ratz, Phys. Lett. B **544**, 1 (2002) [arXiv:hep-ph/0206078].
- [106] T. Miura, T. Shindou and E. Takasugi, Phys. Rev. D **68**, 093009 (2003) [arXiv:hep-ph/0308109]; T. Shindou and E. Takasugi, Phys. Rev. D **70**, 013005 (2004) [arXiv:hep-ph/0402106].
- [107] J. Chakraborty, A. Dighe, S. Goswami and S. Ray, Nucl. Phys. B **820**, 116 (2009) arXiv:0812.2776 [hep-ph].
- [108] F. Vissani, arXiv:hep-ph/9708483; V. D. Barger, S. Pakvasa, T. J. Weiler and K. Whisnant, Phys. Lett. B **437**, 107 (1998) [arXiv:hep-ph/9806387]; A. J. Baltz, A. S. Goldhaber and M. Goldhaber, Phys. Rev. Lett. **81**, 5730 (1998) [arXiv:hep-ph/9806540]; M. Jezabek and Y. Sumino, Phys. Lett. B **440**, 327 (1998) [arXiv:hep-ph/9807310]; G. Altarelli and F. Feruglio, Phys. Lett. B **439**, 112 (1998) [arXiv:hep-ph/9807353];
- [109] Z. Z. Xing, Int. J. Mod. Phys. A **19**, 1 (2004) [arXiv:hep-ph/0307359].